



Research paper

Indole based antimalarial compounds targeting the melatonin pathway: Their design, synthesis and biological evaluation

Tania Luthra ^{a,1}, Akshay Kumar Nayak ^{b,1}, Sarpita Bose ^d, Saikat Chakrabarti ^d, Ashish Gupta ^{b,**}, Subhabrata Sen ^{a,c,*}^a Department of Chemistry, School of Natural Sciences, Shiv Nadar University, Dadri, Chithera, Gautam Budh Nagar, Uttar Pradesh, 201314, India^b Department of Life Science, School of Natural Sciences, Shiv Nadar University, Dadri, Chithera, Gautam Budh Nagar, Uttar Pradesh, 201314, India^c Department of Chemistry, SRM University-Amaravati, Andhra Pradesh, 522020, India^d Structural Biology and Bio-Informatics Division, CSIR-Indian Institute of Chemical Biology, 4, Raja SC Mullick Road, Kolkata, West Bengal, 700032, India

ARTICLE INFO

Article history:

Received 30 December 2018

Received in revised form

6 February 2019

Accepted 6 February 2019

Available online 14 February 2019

Keywords:

C₂-aryliminoindole

Oxidative ring opening

Malaria

Melatonin

Molecular docking

ABSTRACT

Malaria, one of the most severe global diseases, infects nearly 300 million people causing death of about a million population annually. Herein we have reported design, synthesis and biological evaluation of potent antimalarial compounds that target melatonin hormone as a potential pathway for the inhibition of the parasite proliferation. The molecular design is based on melatonin and indole based synthetic and natural antimalarial agents. The library of compounds was accessed *via* an iodine catalyzed one pot organocatalytic ring opening of 1-aryltetrahydro- β -carbolines followed by *in situ* imination of the resulting C₂-aroyl intermediates. Inhibition of parasite growth progression (3D7 and chloroquine resistant RKL9 strain) in the presence of the tested compounds indicated that few of the compounds substantially inhibited the parasite survival and the most potent compound **2j** blocked the parasite growth at the trophozoite stage. Compound **2j** also disrupted the melatonin induced synchronization of the parasite culture *in vitro*. The active compounds were screened against melatonin receptor MT1 to demonstrate substantial binding.

© 2019 Elsevier Masson SAS. All rights reserved.

1. Introduction

Malaria is a global health problem with over 40% of world population living at the risk of the disease [1]. Most of these deaths occur due to infection by *Plasmodium falciparum*. The drugs that are presently applied for the treatment of malaria include artemisinin, pyronaridine, lumefantrine, piperazine, chloroquine, mefloquine, pyrimethamine and atovaquone [2–9]. These are mainly chemotherapeutic drugs. Unfortunately, no reliable vaccine is available for malaria and gradually the parasite is gaining resistance to the aforementioned drugs. This emphasized the urgency in the development of new therapeutic approaches to counter malaria.

All pathogenic symptoms of malaria are associated with the blood stage of parasite life cycle [10], where parasites at merozoite stage invade red blood cells, multiply intracellularly and egress after rupturing red blood cells to re-start the invasion process [11]. Screening of drugs for inhibition of asexual stages of *P. falciparum* is now considered a much more effective strategy than molecular target based approaches [12–18]. The discovery of new antimalarial agents involve development of transmission blocking drugs (TBD) which focus primarily on the blood schizonticides that effectively act against late stage gametocytes [19]. Overall aim of recent day antimalarial drug development has been extermination of all asexual blood stage forms of the parasite. One of such strategies investigated the involvement of melatonin in the intraerythrocytic cycle of malaria parasite [20].

Melatonin (N-acetyl-5-methoxytryptamine), a hormone secreted from pineal gland of all mammals, and also present in some plants partakes in variety of body functions *viz.* immunoregulation, free radical scavenging and sleep and circadian rhythm and regulation [21]. Melatonin inhibitors are also potent anticancer agents, protect organisms against bacterial and viral infection and

* Corresponding author. Department of Chemistry, School of Natural Sciences, Shiv Nadar University, Dadri, Chithera, Gautam Budh Nagar, Uttar Pradesh, 201314, India.

** Corresponding author.

E-mail addresses: ag315@snu.edu.in (A. Gupta), subhabrata.s@srmap.edu.in (S. Sen).

¹ Equal Contributors.

had exhibited reversal symptoms against septic shock [22]. There is an evidence that circadian alteration of melatonin concentration is connected to the synchronous maturation of *Plasmodium falciparum* in human blood [23]. Under *in vitro* condition, melatonin incites parasitemia via activation of melatonin receptors in conjunction with phospholipase-C activation and increment of intracellular Ca^{2+} concentration. Evidently, Ca^{2+} signaling is critical to activate the parasite transition from trophozoite to the schizont stage, thereby promoting parasitemia [24].

Interestingly, despite these revelations there is a dearth of reports involving discovery of potent antimalarials with melatonin as targets. Few notable mentions include pinealectomy or administration of luzindole, a selective melatonin receptor blocker *in vivo* in Balb/C mice that successfully demonstrated the disruption of the parasitic cell cycle [24]. In another study, melatonin derived synthetic indoles inhibited the growth of *P. falciparum* in low micromolar IC_{50} (3–5 μM) [25].

Herein we have reported C_2 -arylimino tryptamine derivatives as novel class of melatonin receptor antagonists (MT1), which have demonstrated substantial antimalarial properties by inhibiting the trophozoite stage of the parasitic life cycle (3D7 strain of *P. falciparum*). The synthesis of the compounds was accomplished via a one pot molecular iodine catalyzed oxidative ring opening of 1-aryltetrahydro- β -carbolines in presence of *tert*-butylhydroperoxide (TBHP) as oxidant and their subsequent imination with primary amines. Experiments demonstrated that the most potent compound of our library works in a fashion similar to luzindole where it inhibits melatonin's action on synchronization of parasitic

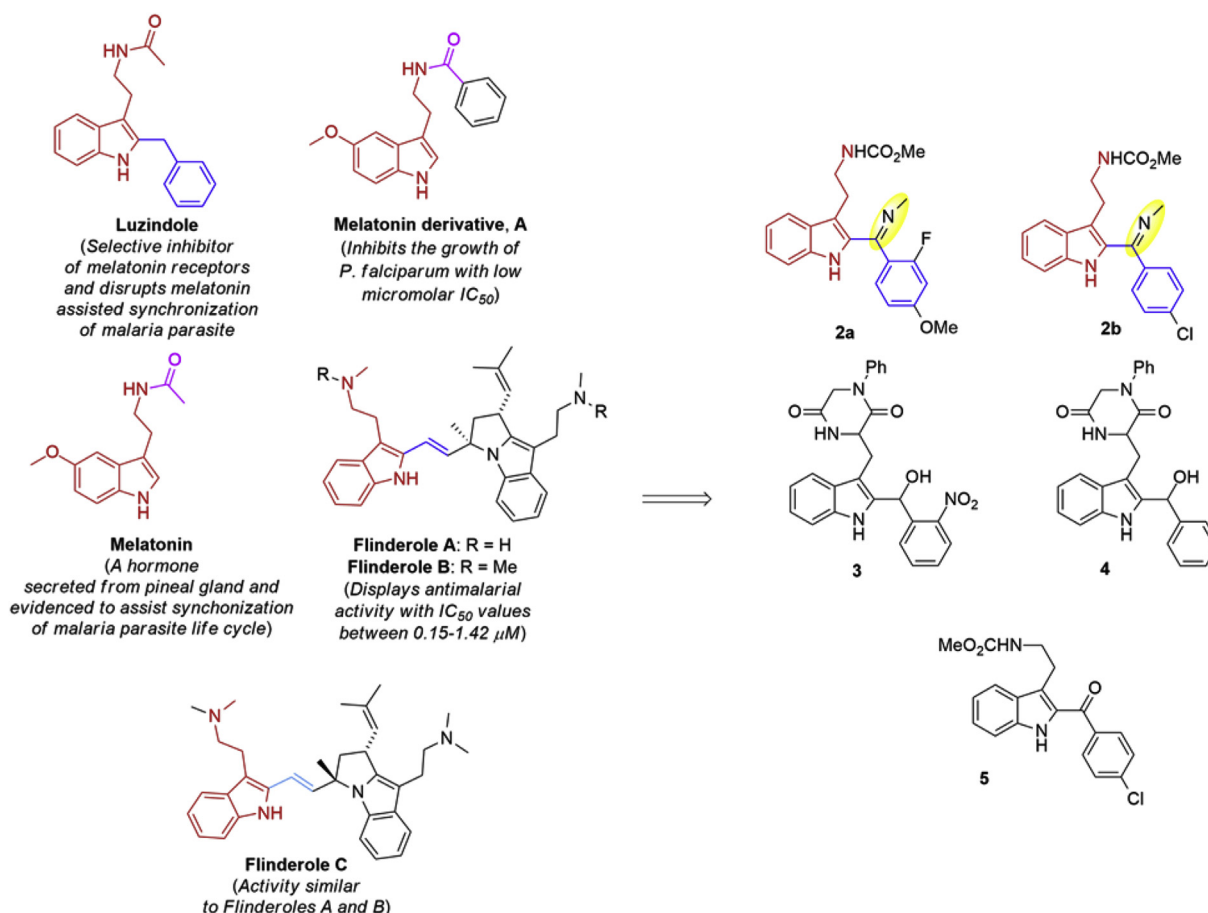
life cycle probably by binding to melatonin receptor MT1.

2. Results

2.1. Design and preliminary screening

A close scrutiny of the indole containing modulators of *P. falciparum* such as melatonin, luzindole, melatonin derivatives, **A**, and flinderoles A–C, reveals that a C_2 substituted tryptamine scaffold is essential to impart modulatory activity in malaria parasite (Scheme 1). Melatonin modulates malaria in a complicated fashion, where in one hand it stimulates growth by influencing the synchronization of the parasite life cycles, on the other hand at high concentration it inhibits the apoptosis and hepato-toxicity caused from the oxidative stress induced by the parasite [26,27]. Luzindole, a selective melatonin receptor antagonist, inhibits the effect of melatonin on synchronization of the erythrocytic cycle of the malaria parasite and thereby arrests their growth [28]. Melatonin derivatives, **A**, were evaluated for their *in vitro* antimalarial activity against 3D7 strain of *P. falciparum* and it was observed that it could block the effect of melatonin in *Plasmodium falciparum*, but could not inhibit the cycle of parasite [25]. Finally, flinderoles A–C, displayed substantial inhibition of the proliferation of the growth of the 3D7 strain of *Plasmodium falciparum* with IC_{50} ranging from 0.08 to 1.42 μM (Scheme 1) [29].

Taking a cue from these structures we initially designed a focussed library of molecules **2a–b**, **3**, **4** and **5** as potential antimalarial compounds which could be melatonin receptor inhibitors



Scheme 1. Design of novel antimalarial compound that could potentially target melatonin hormone.

and therefore could elicit their response by interfering in melatonin induced synchronization of the parasite life cycle (Scheme 1). The newly designed molecules have tryptamine as building block and were protected with carbomethoxy or acetyl groups at the primary nitrogen group of tryptamine. In one of the compounds, a diketopiperazine is tethered to the indole moiety. Inspired from luzindole it was interesting to investigate the antimalarial effect of diverse functionalities at the C₂ position of the indole (Scheme 1). Consequently hydroxy, carboxy and imine moieties were installed resulting in compounds **2a/b** and **3–5**.

An inhibition assay of these compounds at 5 μM, against 3D7 strain of *Plasmodium falciparum* indicated that compound **2b** was most potent, exhibiting nearly 47% of inhibition of proliferation of the parasite (Table 1). Luzindole at 5 μM, showed 48% of inhibition in parasetimia.

This preliminary *in vitro* screening emphasized the importance of the C₂-arylimino moieties in imparting antagonistic modulation on 3D7. This further entrenched that the antimalarial activity demonstrated by **2b** could happen *via* its interference with the melatonin induced synchronization of the parasite life cycle. Based on these results we designed a library of C₂-aryliminotryptamine derivatives.

2.2. Reaction optimization

In a bid to access our desired molecules we envisioned an oxidative ring opening and *in situ* imination of 1-aryl-tetrahydro-β-carbolines. We had already reported a similar procedure for accessing these compounds with iodine and hydrogen peroxide [30]. Herein we wanted to utilize TBHP (tetrabutyl hydrogen peroxide), which is a more controlled oxidant over H₂O₂. Accordingly we began our endeavour with optimization of the reaction conditions (as depicted in Table 2) for the oxidative ring opening of 1-aryl-N-carbomethoxytetrahydro-β-carboline **1a** and the

corresponding imination of the intermediate **1a'** with methyl amine in presence of various iodine sources as catalyst and TBHP as oxidant. The desired C₂-iminomethyl indole derivative **2a** was obtained in good yield when we deployed 0.1 equiv. of molecular iodine and four equiv. of TBHP at 40 °C (entry 1–3). From the initial experiments it was imperative that both molecular iodine and TBHP were necessary (entries 4 and 5). We increased the amount of molecular iodine to 0.3 equiv. which generated the desired product **2a** in 95% yield (entry 6). Exploring the reactions with various other iodine sources did not afford the desired compounds in better yields than molecular iodine (entry 7–10). Hence the optimized protocol for the synthesis of **2a** involved heating a reaction mixture of 0.3 equiv. of iodine with TBHP (4 equiv.) and with methyl amine as the source of nitrogen at 40 °C for about 4 h.

2.3. Synthesis of the library of compounds

With the optimized protocol in hand, a library of C₂-alkaneiminoaryl tryptamine derivatives **2b–p** were synthesized (Table 3). Initial reactions with diversely protected carboline nitrogen indicated that carbomethoxy protected tetrahydrocarbolines **1b–l**, are far more amenable in yielding the desired oxidative products **2b–p** compared to the acetyl or trifluoroacetyl protected analogs, **1m** and **1n** respectively (Table 3). Oxidative ring opening and imination of **1m** lead to multiple spots with ~8% (by LCMS) formation of the desired product **2q** and **1n** afforded the ring dehydrogenated product **2r'** and **2s'** caused by early deprotection of the trifluoroacetyl moiety from the substrate (Table 3). In general, the reactions of **1b–l** provided the desired compounds **2b–p** in moderate to excellent yield (Table 3). Both methyl, ethyl and *n*-propyl amines are used in this generic study. The reaction was equally amenable towards both electron withdrawing and electron donating moieties at the C₁ aromatic ring of the tetrahydrocarboline substrates **1b, c, h–j, l** and **d–g** respectively, as well as the

Table 1

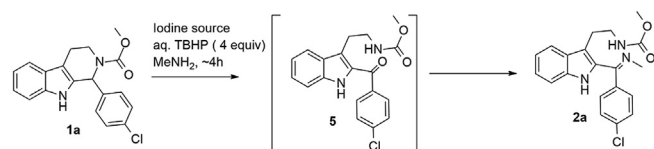
In vitro screening of **7a–e** against 3D7 strain of *Plasmodium falciparum*^a.

Compounds	Luzindole	2a	2b	3	4	5
3D7 inhibitory activity @ 5 μM (% inhibition)	48 ± 0.32	32 ± 0.11	47 ± 0.04	04 ± 0.23	12 ± 0.11	09 ± 0.04

^a The results are an average of three experiments done in triplicates.

Table 2

Exploring reaction conditions for oxidative ring opening and *in situ* imination of **1a**^a.



Entry	Iodine source (equiv)	Temp. (°C)	Yield of 2a (%) ^b
1	I ₂	r. t.	21
2	"	40	39
3	"	60	48
4	-	40	-
5 ^c	I ₂	"	8
6	"	"	95
7	Bu ₄ NI	"	68
8	NaI	"	14
9	MgI ₂	"	62
10	KI	"	12

^a Reaction condition: **1a** (1 mmol), iodine source, TBHP (4 equiv.) for ~4 h.

^b Isolated yields.

^c The reaction was performed without TBHP.

Table 3
Synthesis of library of 2-arylalkanimino tryptamine derivatives, **2b-p**.

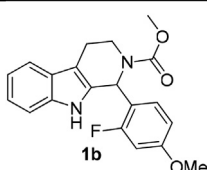
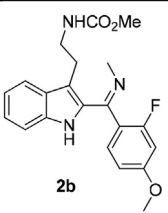

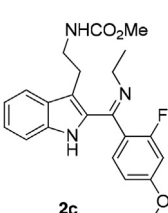
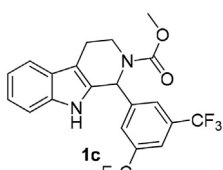
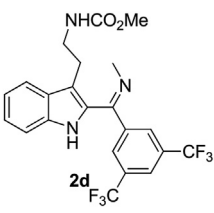
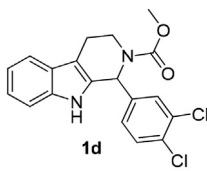
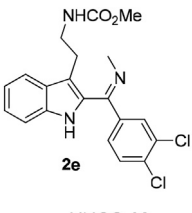
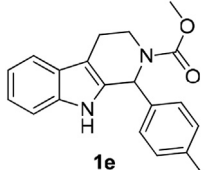
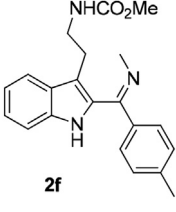

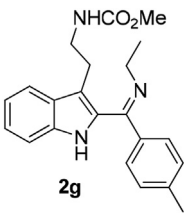
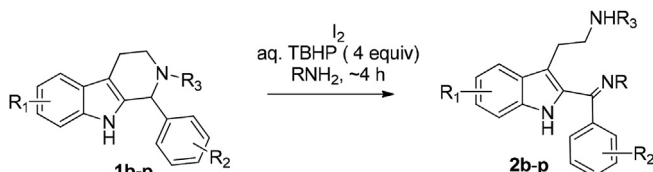
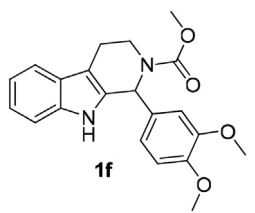
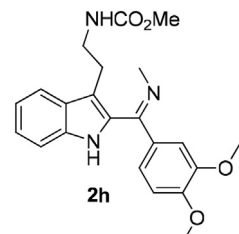
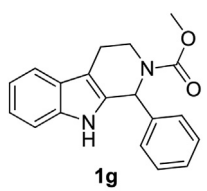
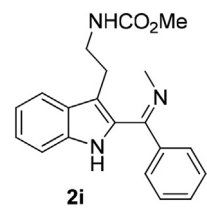
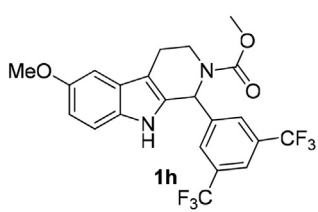
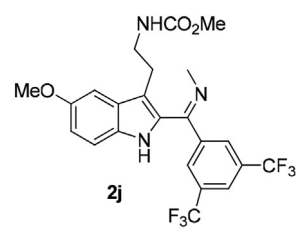
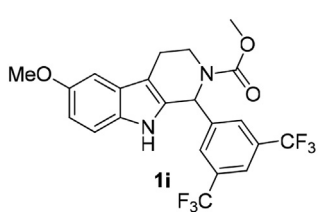
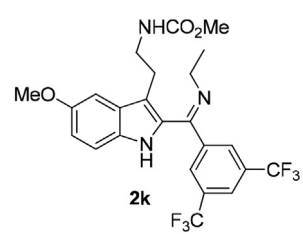
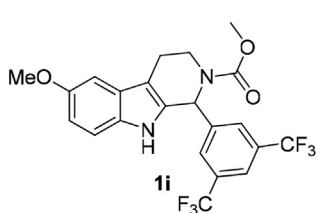
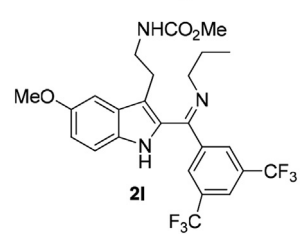
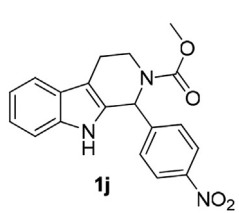
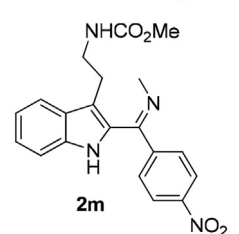
Entry	Substrate (1b-p) ^a	Amines (RNH ₂)	Product	Yield ^b
1	 1b	MeNH ₂	 2b	72
2	 1b	EtNH ₂	 2c	67
3	 1c	MeNH ₂	 2d	82
4	 1d	MeNH ₂	 2e	71
5	 1e	MeNH ₂	 2f	64
6	 1b	EtNH ₂	 2g	88

Table 3 (continued)

Entry	Substrate (1b-p) ^a	Amines (RNH ₂)	Product	Yield ^b
				
7	 1f	MeNH ₂	 2h	84
8	 1g	MeNH ₂	 2i	73
9	 1h	MeNH ₂	 2j	91
10	 1i	EtNH ₂	 2k	76
11	 1i	n-PrNH ₂	 2l	81
12	 1j	MeNH ₂	 2m	65

(continued on next page)

Table 3 (continued)

Entry	Substrate (1b-p) ^a	Amines (RNH ₂)	Product	Yield ^b
13		EtNH ₂		73
14		MeNH ₂		71
15		MeNH ₂		69
16 ^c		MeNH ₂		8
17		MeNH ₂		32
18				41

^a The reactions were conducted at 300 mg of tryptamine and its derivatives.

^b Isolated yield.

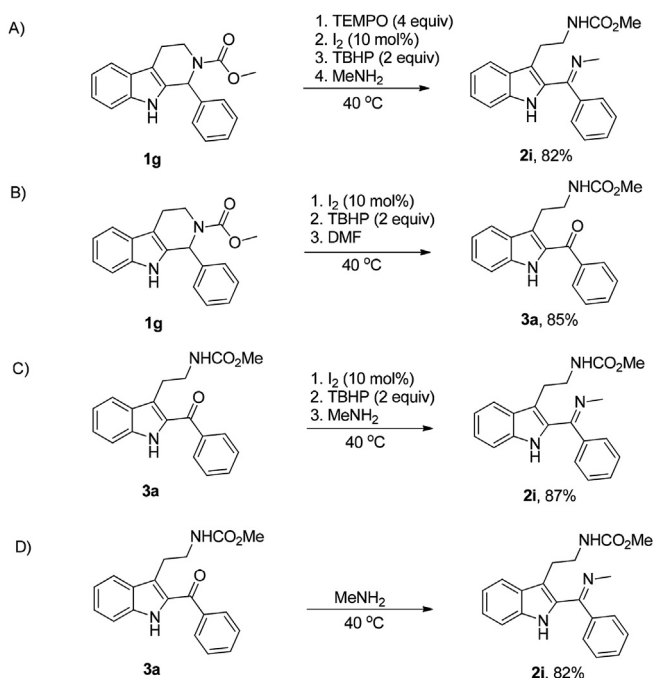
^c Yield by LCMS.

heteroaromatic substituted substrate **1k**. The tetrahydro- β -carbolines **1a-n** were accessed via standard literature protocols and were utilized without purification.

2.4. Reaction mechanism

To perceive the reaction mechanism, several control

experiments were executed at 40 °C. Reaction of **1g** in presence of radical scavenger TEMPO (2, 2, 6, 6-tetramethylpiperidine-N-oxyl) did not influence the product yield of **2i** and a TEMPO-bound adduct was also not observed. This suggested that the reaction probably followed an ionic pathway (Scheme 2A). During the reaction optimization studies, it was noticed that both iodine and TBHP (oxidant) were essential for the reaction and the yield of the



Scheme 2. Control experiments to provide the mechanism.

corresponding products dropped significantly in absence of either of them (Table 1, entry 4 and 5). Additionally, when **1g** was reacted under standard reaction condition but in absence of amines we isolated C₂-aroyl indole **3a** in 85% yield (Scheme 2B). We also wanted to ensure that the C₂-functionalized indole derivatives **2a–n** indeed resulted from imination of the resulting C₂-aroyl indoles. Accordingly, the C₂ aroyl indole derivative **3a**, was treated with methyl amine in presence and absence of molecular iodine (0.1 equiv) and TBHP (2 equiv) (Scheme 2C and 2D). In both cases the

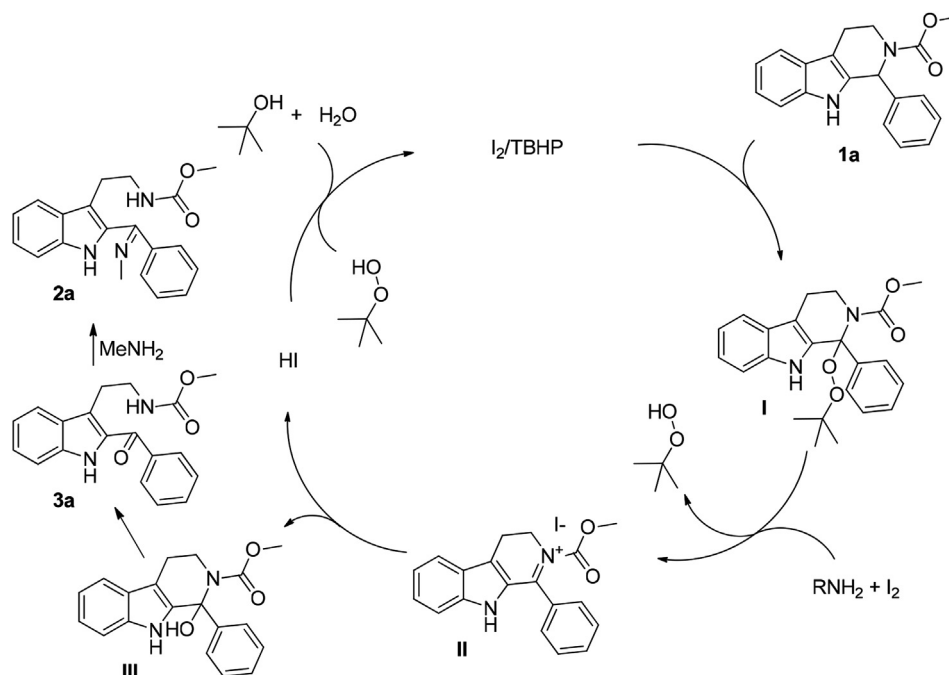
desired compound **2i** was obtained in excellent yield of 87 and 82% respectively.

A mechanism of reaction was proposed in Scheme 3, were in presence of catalytic molecular iodine, 1-aryltetrahydrocarbolines react with TBHP to afford the TBHP coupled intermediate **I**. Next, intermediate **I** was converted to intermediate **II** which then further reacts with the water in the reaction mixture to generate the intermediate **III**. Formation of the C₂ aroyl product **3a** is prompted by the ring opening of the carboline **III** and subsequent imination of **3a** resulted in the formation of **2a** (Scheme 3).

2.5. Compound **2g**, **2i**, **2j**, **2k** and **2p** shows significant parasite growth inhibition and death in 3D7 strain of *P. falciparum*

Next we investigated the ability of our compounds in suppressing the growth of the parasite. Accordingly ring stage synchronized parasite culture (at 1% parasitemia) was treated with **2a** – **2q** at 10 μM concentration for 48 h (Fig. 1b). From the Giemsa staining result for stage specific progression and parasitemia it was revealed that compound **2g**, **2i**, **2j**, **2k** and **2p** of our library could significantly inhibit the growth of *P. falciparum* (Fig. 1b). Compound **2j** demonstrated the strongest inhibition (Fig. 1b). Compounds **2g** and **2j** blocked the parasite growth progression mainly in trophozoite stage while compounds **2i**, **2k** and **2p** did not show any significant stage-specific inhibition (Fig. 1c). Luzindole, inhibitor of melatonin receptors, was used as a positive control, and it exhibited parasite growth inhibition compared to the control (DMSO).

To identify the IC₅₀ value of the selected compounds, synchronized ring stage parasite culture were treated with 1, 5, 10, and 20 μM concentration of compounds for 48 h and parasitemia was calculated. IC₅₀ value of compound **2g**, **2i**, **2j**, **2k**, and **2p** were found to be 4.28 μM , 0.89 μM , 0.74 μM , 2.73 μM and 0.73 μM respectively (Fig. 2). It is also noteworthy that these compounds when screened against mammalian HepG2 cell line evoked negligible cytotoxic response at 5 μM concentration (0.2 → 12% inhibition), rendering them non cytotoxic against mammalian cells (refer Supplementary Information).



Scheme 3. Reaction mechanism of HCDC mediated oxidative ring opening of THCs with amines.

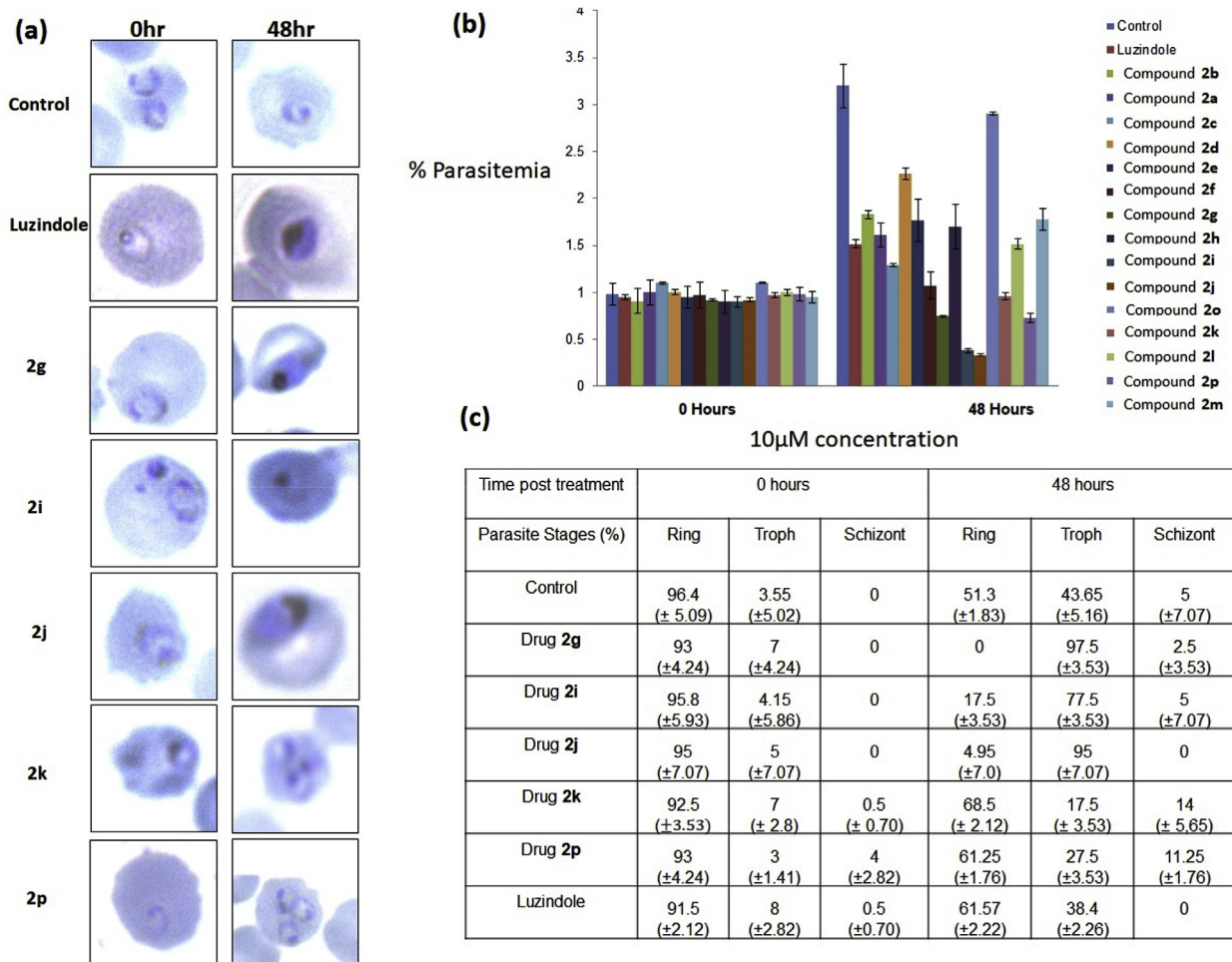


Fig. 1. (a) Giemsa staining data for the effect of compounds **2g**, **i**, **j**, **k** and **p** on stage specific progression of the parasite. (b) Effect of compounds on parasite growth. Ring stage synchronized culture were treated with indicated compounds at 10 μM concentration and parasitemia was calculated at 0 and 48 h post treatment. Value shows average from three independent experiments with $\pm\text{SD}$ (@ 10 μM). (c) Percentage of surviving parasites at different stages at 0 and 48 h post-treatment of indicated compounds at 10 μM concentration. Value shows average from three independent experiments with $\pm\text{SD}$.

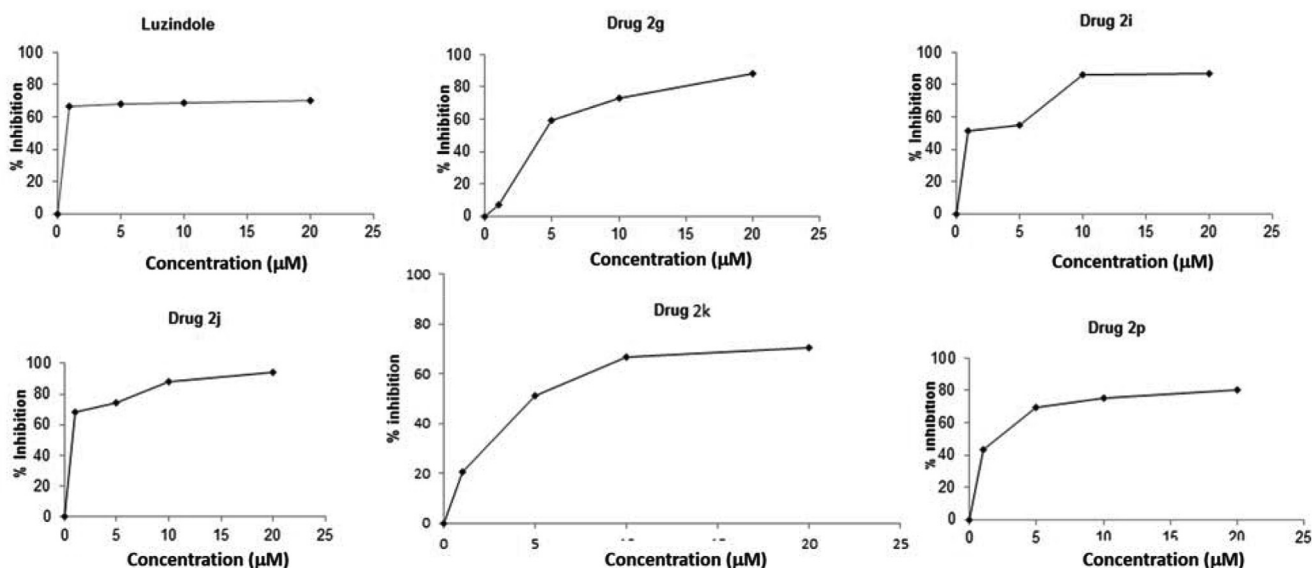


Fig. 2. (a) Dose response curve of compounds **2g**, **i**, **j**, **k** and **p** against 3D7 (* $P < 0.05$ vs control (untreated cells)).

2.6. Compound **2g**, **2i**, **2j**, **2k** and **2p** shows significant parasite growth inhibition and death in CQ-resistant RKL9 strain

Next we evaluated the biological activity of the most active compounds of our library i.e. **2g**, **2i**, **2j**, **2k** and **2p** against the chloroquine (CQ)-resistant, RKL9 strain of *P. falciparum*. Accordingly these compounds were screened in a dose response manner and the results were plotted as % parasitemia versus time, over a range of concentration (1 μ M–20 μ M) (Fig. 3) for both 3D7 and RKL9 strains. A close scrutiny of the results revealed that in general the compounds are efficacious against RKL9 in a dose response manner and showed significant parasite death. However it is worth mentioning that when compared to 3D7, the overall inhibitory potency of these compounds against RKL9 strain were slightly less. Among the compounds screened, as expected compound **2j** was

most potent followed by **2p** and **2i**.

Some reports have shown that melatonin can promote parasite growth and can induce synchrony of parasite culture.¹⁷ We treated parasites with melatonin and found that melatonin treatment can induce parasitemia as well as synchronization of parasites compared to control treated parasites under *in vitro* conditions (Tables 3a and 3b).

Next we investigated whether our compounds could interfere with the melatonin pathway. Accordingly mixed stage parasite culture were either treated with melatonin, melatonin/luzindole (control compound) and melatonin/compound **2j** (test compound) for 48 h. Subsequently parasitemia was monitored 48 h post-treatment.

Interestingly, our results showed that both luzindole and **2j** can decrease melatonin induced parasitemia of malaria parasite

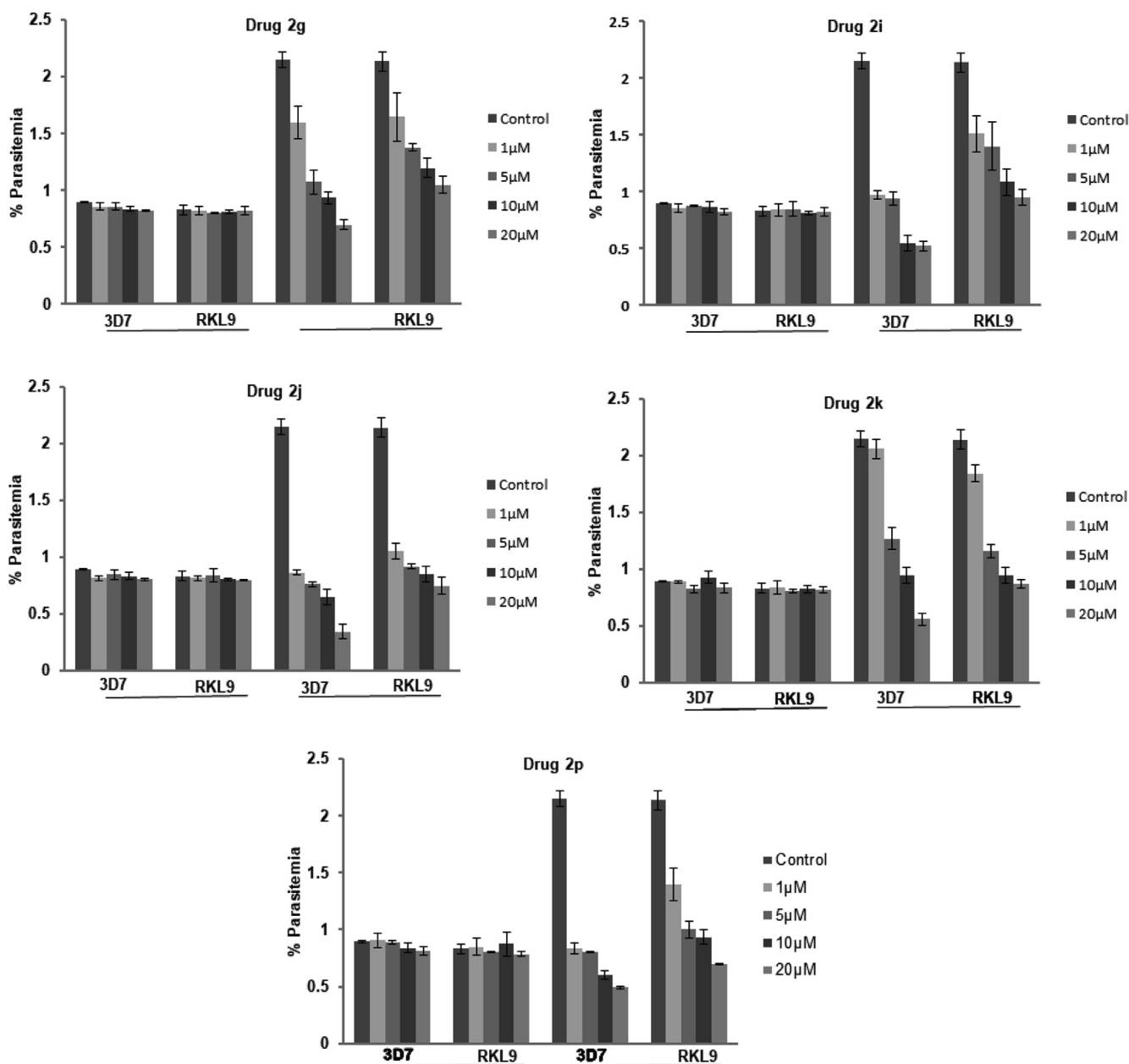


Fig. 3. Screening of compounds **2g**, **2i**, **2j**, **2k** and **2p** against CQ-resistant RKL9 strain. Synchronized parasite culture of both 3D7 and RKL9 strain were treated indicated compounds for 1, 5, 10 and 20 μ M concentration. Graph were plotted for parasitemia measured at 0 and 48 h. Values shows average of three independent experiments with \pm SD. Compound **2j** can disrupt melatonin-induced synchrony of Plasmodium culture *in vitro*.

Table 3a
Effect of 2j and melatonin on parasitemia.

Time post treatment	0 h	48 h
Parasitemia (%)		
Control	1.10 (±0.14)	3.57 (±0.45)
Melatonin 1 μM (M2)	1.05 (±0.07)	4.76 (±0.61)
M2 + Luzindole 1 μM	1.10 (±0.14)	2.88 (±0.37)
M2 + Luzindole 5 μM	1.03 (±0.10)	2.56 (±0.32)
M2 + 2j 1 μM	1.15 (±0.07)	2.80 (±0.14)
M2 + 2j 5 μM	1.10 (±0.14)	1.65 (±0.21)

(luzindole (1.11 → 2.88 [@ 1 μM] and 1.025 → 2.25 [5 μM]) and 2j (1.15 → 2.8 [@1 μM] and 1.1 → 1.65 [@ 5 μM]) (Table 3a). There is significant decrease in parasitemia in presence co-treatment of parasites with melatonin and 2j compared to melatonin alone and it further decreases with increasing concentration of 2j compound. Similar results were obtained when Luzindazole was used to co-treat parasites with melatonin.

Next, to determine whether there is any effect of 2j compound on melatonin induced synchronization of malaria parasite, stages of the parasite 48 h post treatment were analyzed and result showed that melatonin treatment considerably increases the synchronization of parasites. However presence of either 2j or luzindole disrupts this melatonin induced synchrony of parasites (Table 3b).

Together these results showed that compound 2j could not only negate melatonin-induced parasitemia growth but also can also disrupted melatonin-induced synchrony of human malaria parasite most probably through inhibition of melatonin receptors.

2.7. Investigation with melatonin receptor MT1

In a bid to understand whether our potent antimalarial compounds indeed imposed their inhibitory potential through melatonin receptor, we conducted experiments to investigate the binding ability of compound 2g, j and k against melatonin receptor MT1 (Fig. 4). Melatonin was used as control. It was observed that the increase in concentration of compound 2g from 500 nM → 1 μM → 5 μM hardly imposed any inhibitory effect on the enzyme (Fig. 4). Interestingly, compound 2j and k bound strongly with the enzyme as demonstrated by their high percentage inhibition when interacted with the receptor (Fig. 4). Compound 2j, at 500 nM displayed nearly 75% inhibition which increased to ~85% with the increase in concentration to 5 μM. Compound 2k, also displayed 60% inhibition at 500 nM, which got increased to ~80% at 1 μM, however decreased to 70% at 5 μM (Fig. 4).

2.7.1. Stability of the compound 2g, i, j, k and p

The stability of compounds 2g, 2i, 2j, 2k and 2p was measured by HPLC analysis and it was found that in simulated stomach acid (0.01 N HCl, pH = 2.0 at 37 °C), the compounds 2i, 2j and 2k (1 mg/ml) disappeared and underwent hydrolysis within 24 h of reaction. During this time only 20% of the compound 2g remained.

Table 3b

Effect of compound 2j on melatonin-induced synchronization of the parasite (Value shows average of three independent experiments with ±SD).

Time post treatment	0 h			48 h		
	Ring	Troph	Schizont	Ring	Troph	Schizont
Control	22.50 (±0.70)	52.50 (±0.70)	24.65 (±1.90)	22.25 (±8.83)	70.00 (±9.89)	7.75 (±1.06)
Melatonin 1 μM (M2)	23.90 (±0.84)	52.50 (±0.70)	23.25 (±0.35)	11.80 (±9.19)	88.20 (±9.19)	0.00
M2 + Luzindole 1 μM	23.00 (±1.41)	50.50 (±0.70)	25.80 (±0.70)	19.10 (±10.18)	80.90 (±10.18)	0.00
M2 + Luzindole 5 μM	23.75 (±1.06)	51.90 (±1.97)	24.00 (±1.41)	21.97 (±6.26)	77.15 (±5.02)	0.88 (±1.23)
M2 + 2j 1 μM	24.20 (±0.98)	53.80 (±1.13)	22.95 (±0.07)	18.00 (±0.77)	79.10 (±0.56)	2.90 (±1.84)
M2 + 2j 5 μM	24.10 (±1.27)	53.25 (±2.47)	21.85 (±1.20)	27.25 (±11.38)	70.90 (±10.18)	1.85 (±0.21)

Interestingly it was observed that compound 2p was most stable as ~90% of it was left till 24 h as depicted in Fig. 5a. The stability of compounds were also measured in physiological buffer (pH = 7.4 at 37 °C) by HPLC analysis (Fig. 4b) and it was found that the compounds 2g and 2i disappeared within 24 h of reaction. Nearly 60% of the compounds 2j and k and 95% of 2p was left till 24 h (Fig. 5b). A close scrutiny of the structures of compound 2j (most active) and compound 2p (most stable) revealed that probably compound 2j was less stable because of the presence of electron withdrawing group (-CF₃), which facilitates its hydrolysis while presence of two fluoro group at the *ortho* position of compound 2p makes its stable towards hydrolysis.

2.8. Molecular docking of 2j and 2k

Fig. S1 (supplementary information) provides the outline of molecular modelling and docking study. Fig. 6 shows the docking orientation of the compounds 2j and 2k with respect to the human MT1 homology model generated via MODELLER [31]. Compounds 2j and 2k were docked onto the previously suggested binding pocket of MT1 and most plausible docking solutions for each compound were chosen via root mean square deviation (RMSD) based clustering and docking scores [32]. The protein-ligand complexes were further considered for the interaction analysis and the probable interacting residues are marked in Fig. 5 and also listed in Table S1. Docking properties of compounds 2j and 2k were further compared with the same obtained from docking of melatonin receptor agonist 2-phenylmelatonin (2PhMLT). Docking score represented as GOLD fitness score and the ΔG of binding are found to be higher for compounds 2j and 2k compared to 2PhMLT (Table 4).

3. Discussion

Melatonin, the hormone produced in the pineal gland of the brain is known to modulate the sleep cycle and circadian rhythm in humans. It acts through melatonin receptors M1 and M2. Interestingly, some reports have shown that melatonin helps in parasite survival by scavenging the ROS and can also promote parasite synchronization [23]. A library of C₂-substituted tryptamine derivatives, 2a, b, 3–5 was designed from melatonin, luzindole (selective melatonin receptor inhibitor), melatonin derivatives 3 and antimalarial flinderoles. Preliminary screening against 3d7 strain of *P. falciparum* revealed that compound 2b a C₂-arylimino tryptamine derivative imposed maximum inhibition (47%) (Table 1) to the proliferation of the parasite. Luzindole, the +ve control inhibited the parasite with ~48% inhibition. From these initial results a library based on 2b was designed. An iodine catalyzed oxidative ring opening and *in situ* imination with appropriate amines of 1-aryltetrahydro-β-carbolines provided access to the desired molecules, 2a - p. *In vitro* screening of 2a - p against 3D7 and CQ-resistant RKL9 strain of *P. falciparum* showed that some of these compounds (2g, 2i, 2j, 2k and 2p) could cause significant death of

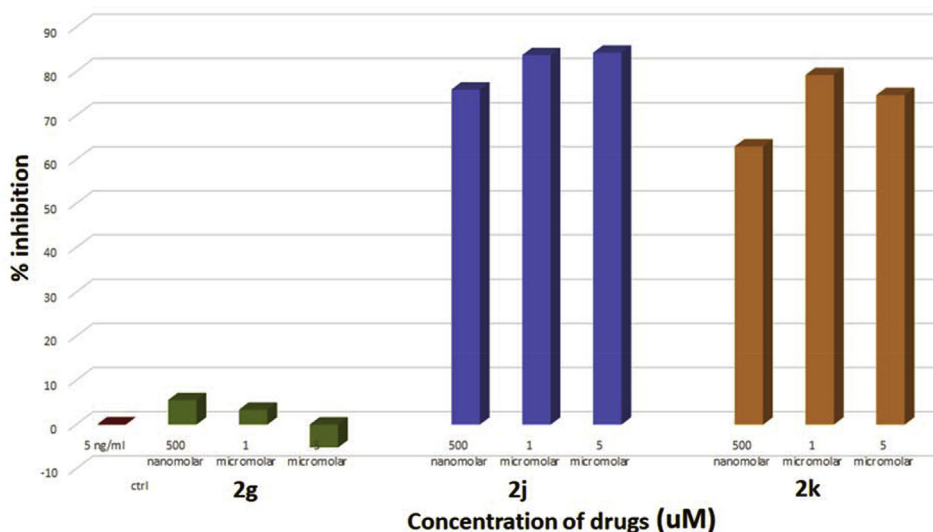


Fig. 4. Binding study of 2g, 2j and 2k with MT1. *P < 0.05 relative to control.

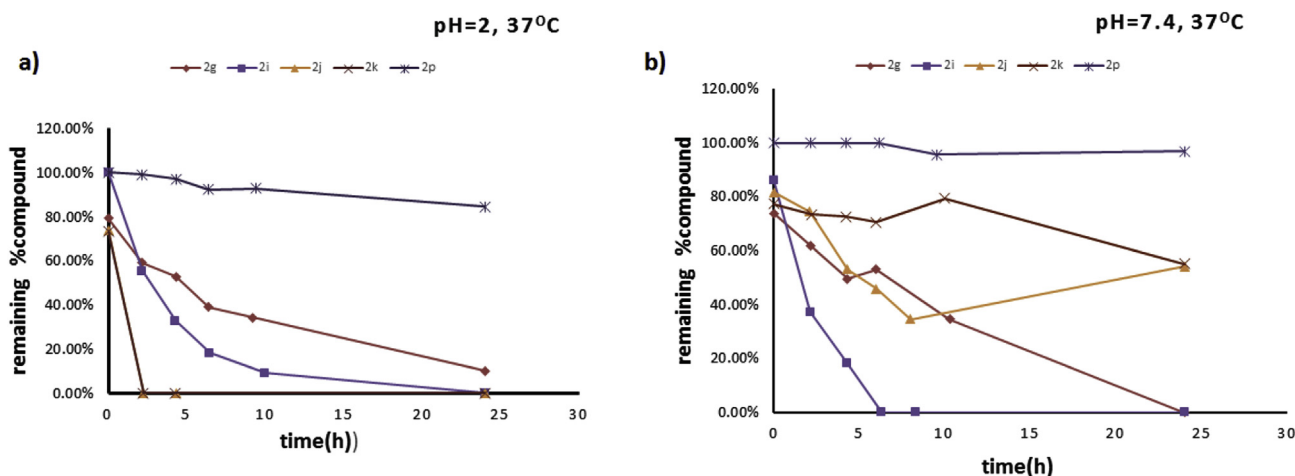


Fig. 5. Time course stability of compound 2g, 2i, 2j, 2k and 2p at pH (a) 2 in HCl and b) 7.4 in phosphate buffer maintained at 37 °C.

these strains under *in vitro* conditions (Fig. 3). Since one of the major problems associated with malaria is the resistance that the *P. falciparum* develop towards the antimalarials, discovery of such efficacious indole based small molecules like ours against CQ-resistant RKL9 strain further highlight the importance of our compounds.

To assess the structure activity relationship (SAR) the general molecular architecture of our compound library was divided into three segments, A, B and C as depicted in Fig. 7. The segment A comprised of the benzene ring connected to the C₂ position of the indole ring through an imine linker (Fig. 7). Herein various electron donating substituents such as methoxy, chloro and methyl at the 4-position of the benzene ring evoked antimalarial activity for the compounds. Interestingly any substitution at the 3-position was detrimental. Electron withdrawing substitution at the 2-position improved the inhibition. This was exemplified by comparison of the antiparasitic activity of the compounds, **2d** < **2b** ≤ **2h** ≤ **2e** < **2a** < **2f** ≤ **2c** < **2g** < **2p** (Fig. 1b). The next trend is observed in segment B and C, as displayed by the 3, 5-bis-trifluoromethyl substituted analogs, **2d**, **l**, **k** and **j**. Herein the methoxy substitution at C₅-position of the indole for **2l**, **k** and **j** enhanced the activity by two to

four times of the corresponding analogs compared to the unsubstituted **2d** (Fig. 1b). Interestingly among these analogs the activity reduced drastically from N-methyl → ethyl → *n*-propylated analog (**2j** > **2k** > **2l**). This apparently contradicted the trend observed for **2b/e** and **2f/g** where ethyl substituted **2e** and **g** were almost twice and 1.5 times more active than the methylated analogs **2b** and **f** respectively (Fig. 1b). The only heteroaryl, 4-bromothiophenyl analog **2o** exhibited poor inhibitory properties against the parasite (15% inhibition). Compound **2i**, with no substitution in segment A and C exhibited profound inhibition of parasitemia.

The most active compound **2j** could disrupt melatonin-induced synchrony of parasite culture similar to luzindole (Fig. 2a/b). *In vitro* screening against melatonin receptor MT1 demonstrated that our compounds **2j** and **k**, binds effectively with the receptor (Fig. 3) and the binding interaction improves with the increase of concentration of the molecules from 0.5 → 5 μM. This observation rationalized the results depicted in Fig. 2a/b, where, by potentially blocking melatonin receptors compound **2j** can negate the effect of melatonin which consequently results in less synchrony of parasite culture in presence of the compound. However, since compound **2j** demonstrated blockage of parasites in trophozoite stage, it might

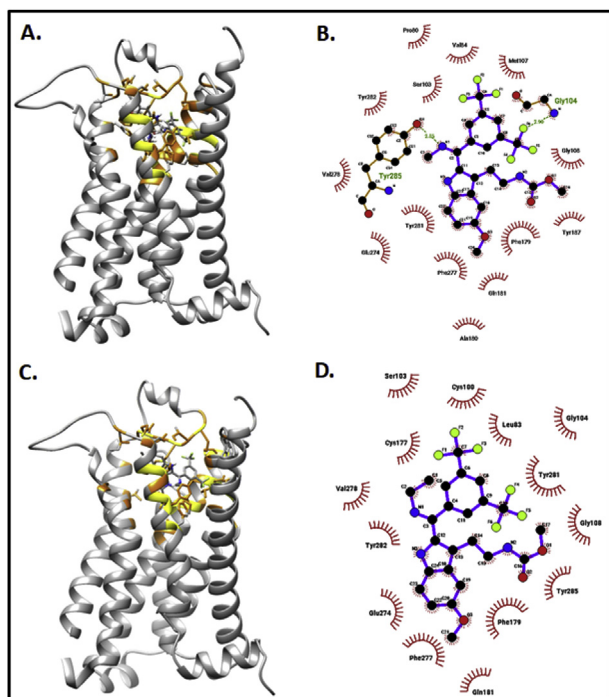


Fig. 6. Docking orientation and the probable interacting residues are shown for compound **2j** (A and B) and compound **2k** (C and D), respectively. MT1 residues residing within 5 Å and 2.5 Å of the docked ligands are shown in orange and yellow, respectively. Interaction plots were generated using the LigPlot program [33].

Table 4
Comparison of the docking properties.

Compound	GOLD Fitness Score	ΔG of Docking	Avg. GOLD Fitness Score	Avg. ΔG of Docking
2j	76.18	-16.73	75.86	-16.45
2k	78.62	-17.09	77.88	-17.02
2PhMLT	63.53	-12.43	62.59	-12.71

be possible that it could have multiple targets apart from melatonin receptors, which are specifically expressed in trophozoite stage and are essential for stage progression in schizont stage during intraerythrocytic developmental cycle (IDC). Finally, molecular docking

experiment of **2j** and **k** against a homology model of MT1 revealed putative binding interaction (as depicted in Fig. 6 and Table S1 [supplementary information]) that further substantiated our *in vitro* binding studies against MT1.

4. Conclusion

Herein we reported discovery of a novel class of antimalarials based on C_2 -arylalkanimino tryptamine derivatives. These compounds were designed based on melatonin and related compounds. Preliminary antimalarial screening rationalized the molecular design. The compound library was synthesized by iodine catalyzed oxidative ring opening of 1-aryltetrahydro- β -carbolines **1a-n** and *in situ* imination of the resulting C_2 -aroyl intermediates in presence of appropriate amines. The mechanism of the transformation was proposed based on control experiments. Compound **2a-p** exhibited moderate to substantial antimalarial activity against 3D7 strain of *P. falciparum*. The most active compounds in the series, **2g**, **i**, **j**, **k** and **p** (IC_{50} of 4.28, 0.89, 0.74, 2.73 and 0.73 μM respectively) inhibited progression of the intraerythrocytic cycle of the parasite primarily at the trophozoite stage and interrupted the melatonin hormone induced synchronization for the parasite growth. Binding studies against melatonin receptor MT1, demonstrated that compound **2j** and **k** binds to the enzyme, and the binding improves with the increase in the concentration of the molecules. Compounds **2g**, **i**, **j**, **k** and **p** were also efficacious against CQ-resistant RKL9 strain. This investigation demonstrated the utility and potency of our molecules as potent antimalarials.

5. Experimental

5.1. Chemistry

General. All reactions were carried out under N_2 atmosphere as specified. The starting material tryptamine, appropriate aldehydes, common reagents like anh. Na_2SO_4 , anh. $MgSO_4$, triethyl amine etc. along with solvents were purchased from Sigma Aldrich. Column chromatography was performed on Silica gel (100–200 mesh) (purchased from Sigma Aldrich), and reactions was monitored by thin layer chromatography (TLC, Silica gel 60 F₂₅₄), using UV light to visualize the course of the reaction. 1H NMR and ^{13}C NMR spectra were recorded with Bruker 400 MHz instruments at 400 MHz for 1H NMR and 100 MHz for ^{13}C NMR spectroscopy with tetramethyl silane as an internal standard at ambient temperature unless otherwise indicated. Splitting patterns are designated as singlet (s),

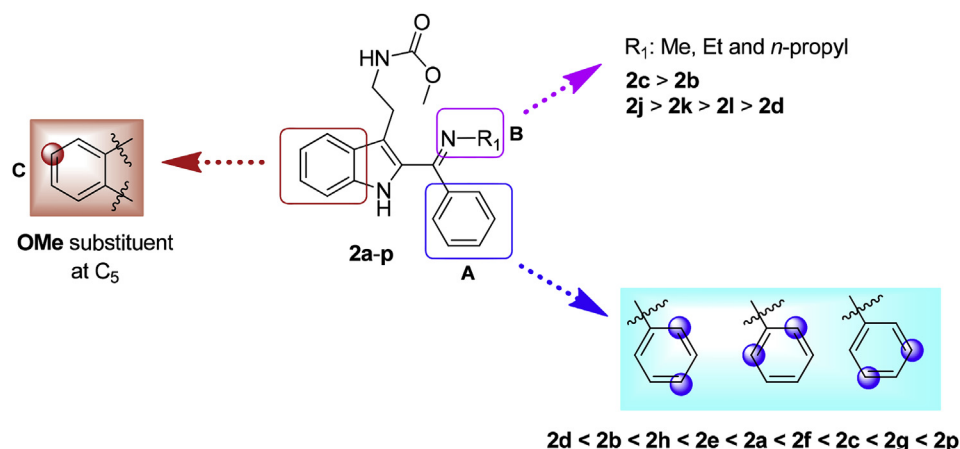


Fig. 7. Structure Activity Relationship (SAR) studies for **2a-p**.

broad singlet (br, s), doublet (d), triplet (t). Splitting patterns that could not be interpreted or easily visualized are designated as multiplet (m). Mass spectrometry analysis was done with a 6540 UHD Accurate-Mass QTOF LC-MS system (Agilent Technologies) equipped with an Agilent 1290 LC system obtained by the Department of Chemistry, School of Natural Sciences, Shiv Nadar University, Uttar Pradesh 201314, India. HPLC experiments were carried out in Agilent Eclipse Plus C18 column.

5.1.1. Synthesis of tetrahydro- β -carbolines **1a-p**

Trifluoroacetic acid (1.5 equiv.) and substituted benzaldehydes (0.8 equiv) were added to the solution of tryptamine or 5-methoxytryptamine (1 equiv.) in dichloromethane (DCM). The resulting mixture was allowed to stir at room temperature for 24 h. Once thin layer chromatography (TLC) confirmed complete consumption of the starting material, the residue was mixed with a 5% K_2CO_3 aqueous solution and extracted with DCM. The organic layer was dried over anhydrous $MgSO_4$ and evaporated under reduced pressure to get the crude product. When the product started to precipitate from DCM, it was filtered off and washed with 5% K_2CO_3 aqueous solution and DCM. This product was used further without further purification.

To a DCM solution of the above unsubstituted tetrahydro- β -carbolines (1 equiv.) (obtained from tryptamine derivatives and appropriate benzaldehydes) in 4 N aq. NaOH solution (1 equiv.) or triethylamine (3 equiv.), methyl chloroformate (1 equiv.) or acetyl chloride (2 equiv.) or trifluoroacetic anhydride (1.1 equiv.) was added dropwise at 0 °C. The reaction mixture was stirred at room temperature under nitrogen atmosphere for 3 h. After complete consumption of the starting material the reaction mixture was diluted with water and extracted with ethyl acetate. The organic layer was washed with saturated solution of $NaHCO_3$ and brine. The organic layer was dried over anhydrous Na_2SO_4 , and evaporated under reduced pressure to obtain a crude product which was taken to the next step without purification.

5.1.2. Oxidative ring opening of **1a-p** for the synthesis of **2a-p**

Compounds **1a-p** (1 equiv.), molecular iodine (0.3 equiv.) and *tert*-butyl hydroperoxide (4 equiv.) were taken in methylamine/ethylamine and were stirred at 40 °C temperature for 4 h. The reaction was monitored by TLC, and after completion the reaction mixture was cooled to room temperature and quenched with saturated solution of $Na_2S_2O_4$ in water and extracted with ethyl acetate. The organic layer was dried over anhydrous $Na_2S_2O_4$, and evaporated under reduced pressure. The crude product was purified by gradient column chromatography with 30–50% ethyl acetate-hexane mixture as eluent.

5.1.3. (*Z*)-methyl(2-(2-((4-chlorophenyl)(methylimino)methyl)-1H-indol-3-yl)ethyl)carbamate (**2a**)

Compound **2a** was synthesized from **1a** as yellow solid, by following the general procedure. It was purified by column chromatography with ethyl acetate-hexane (3:10) mixture as an eluent. The yield of the reaction was 95%. 1H NMR (400 MHz; $DMSO-d_6$) δ 11.48 (s, 1H), 7.79–7.77 (d, $J = 6.64$ Hz, 1H), 7.76–7.75 (d, $J = 5.64$ Hz, 2H), 7.66–7.64 (d, $J = 8.40$ Hz, 2H), 7.44–7.42 (d, $J = 8.32$ Hz, 1H), 7.32–7.30 (m, 1H), 7.13–7.09 (m, 2H), 3.46 (s, 3H), 3.15 (s, 3H), 3.02–2.99 (m, 2H), 2.02–1.99 (m, 2H). ^{13}C NMR (100 MHz; $DMSO-d_6$) δ 161.81, 156.95, 138.22, 136.69, 135.33, 129.70, 129.46, 128.85, 127.52, 122.45, 119.42, 112.03, 51.53, 42.31, 41.22, 25.70. IR (neat, ν cm^{-1}): 3216, 2920, 1693, 1076, 745. m/z : calculated for $C_{20}H_{20}N_3O_2Cl$ $[M+H]^+$: 370.1317 found 370.1315. Melting point: 149 °C

5.1.4. (*Z*)-methyl(2-(2-((2-fluoro-4-methoxyphenyl)(methylimino)methyl)-1H-indol-3-yl)ethyl)carbamate (**2b**)

Compound **2b** was synthesized from **1b** as light yellow solid, by following the general procedure. It was purified by column chromatography with ethyl acetate-hexane (3:10) mixture as an eluent. The yield of the reaction was 72%. 1H NMR (400 MHz; $DMSO-d_6$) δ 10.99 (s, 1H), 7.60–7.58 (d, $J = 7.92$ Hz, 1H), 7.37–7.35 (d, $J = 8.16$ Hz, 1H), 7.22–7.17 (t, $J = 8.32$ Hz, 1H), 7.15–7.11 (m, 2H), 7.02–6.91 (m, 3H); 3.85 (s, 3H), 3.48 (s, 3H), 3.16 (s, 3H), 2.95–2.92 (m, 2H), 2.46–2.44 (d, $J = 7.20$ Hz, 2H); ^{13}C NMR (100 MHz; $DMSO-d_6$) δ 157.91, 156.96, 136.41, 133.50, 130.54, 128.97, 123.78, 119.86, 119.24, 115.23, 112.30, 111.65, 102.53, 56.21, 51.53, 42.10, 24.97. IR (neat, ν cm^{-1}): 3184, 2850, 1688, 1318, 1154. m/z : calculated for $C_{21}H_{22}N_3O_3F$ $[M+H]^+$: 384.1718 found 384.1765. Melting point: 188 °C

5.1.5. (*Z*)-methyl(2-(2-((ethylimino)(2-fluoro-4-methoxyphenyl)methyl)-1H-indol-3-yl)ethyl)carbamate (**2c**)

Compound **2c** was synthesized from **1b** as yellow solid, by following the general procedure. It was purified by column chromatography with ethyl acetate-hexane (3:10) mixture as an eluent. The yield of the reaction was 67%. 1H NMR (400 MHz; $CDCl_3$) δ 8.94 (s, 1H), 7.61–7.59 (d, $J = 7.88$ Hz, 1H), 7.33–7.31 (d, $J = 8.08$ Hz, 1H), 7.26–7.24 (d, $J = 7.92$ Hz, 1H), 7.12–7.06 (m, 2H), 6.82–6.79 (dd, $J_1 = 2.00$ Hz and $J_2 = 6.40$ Hz, 1H), 6.76–6.73 (dd, $J_1 = 2.00$ Hz and $J_2 = 8.88$ Hz, 1H), 3.88 (s, 3H), 3.61 (s, 3H), 3.39 (s, 2H), 3.25–3.24 (d, $J = 4.96$ Hz, 2H), 2.59 (s, 2H), 1.31–1.29 (m, 3H); ^{13}C NMR (100 MHz; $CDCl_3$): 160.25, 141.87, 136.92, 133.02, 131.17, 128.02, 127.42, 126.94, 123.00, 119.74, 112.26, 51.36, 42.60, 41.11, 29.44, 25.47. IR (neat, ν cm^{-1}): 3276, 2918, 1690, 1273, 1130. m/z : calculated for $C_{22}H_{24}N_3O_3F$ $[M+H]^+$: 398.1874 found 398.1865. Melting point: 143 °C

5.1.6. (*Z*)-methyl(2-(2-((3,5-bis(trifluoromethyl)phenyl)(methylimino)methyl)-1H-indol-3-yl)ethyl)carbamate (**2d**)

Compound **2d** was synthesized from **1c** as yellow solid, by following the general procedure. It was purified by column chromatography with ethyl acetate-hexane (3:10) mixture as an eluent. The yield of the reaction was 82%. 1H NMR (400 MHz; $DMSO-d_6$) δ 11.25 (s, 1H), 8.26 (s, 1H), 8.08 (s, 2H), 7.69–7.67 (d, $J = 7.84$ Hz, 1H), 7.41–7.39 (d, $J = 8.08$ Hz, 1H), 7.22–7.18 (m, 1H), 7.12–7.08 (m, 1H), 7.04–7.01 (m, 1H), 3.38 (s, 3H), 3.33 (s, 3H), 3.12–3.08 (m, 2H), 2.64–2.60 (t, $J = 7.04$ Hz, 2H); ^{13}C NMR (100 MHz; $DMSO-d_6$): 160.19, 156.86, 141.81, 136.89, 131.13, 130.80, 128.03, 127.39, 126.91, 124.17, 122.99, 122.26, 119.74, 119.67, 113.16, 112.26, 51.35, 42.61, 41.08, 25.46. IR (neat, ν cm^{-1}): 3270, 2942, 1699, 1635, 1252, 1130. m/z : calculated for $C_{22}H_{19}N_3O_2F_6$ $[M+H]^+$: 472.1454 found 472.1446. Melting point: 162 °C

5.1.7. (*Z*)-methyl(2-(2-((3,4-dichlorophenyl)(methylimino)methyl)-1H-indol-3-yl)ethyl)carbamate (**2e**)

Compound **2e** was synthesized from **1d** as yellow solid, by following the general procedure. It was purified by column chromatography with ethyl acetate-hexane (3:10) mixture as an eluent. The yield of the reaction was 71%. 1H NMR (400 MHz; $DMSO-d_6$) δ 11.20 (s, 1H), 7.75 (d, $J = 1.96$ Hz, 1H), 7.66–7.64 (d, $J = 8.40$ Hz, 2H), 7.42–7.39 (dd, $J_1 = 2.00$ Hz and $J_2 = 6.52$ Hz, 1H), 7.38–7.36 (m, 1H), 7.19–7.13 (m, 1H), 7.09–7.06 (m, 2H), 3.40 (s, 3H), 3.29 (s, 3H), 3.11–3.06 (m, 2H), 2.62–2.58 (m, 2H). ^{13}C NMR (100 MHz; $DMSO-d_6$): 160.75, 156.94, 139.98, 136.76, 133.23, 132.31, 131.79, 131.16, 130.12, 129.14, 128.31, 127.60, 127.46, 122.69, 119.55, 112.42, 112.13, 51.50, 42.44, 41.17, 25.60. IR (neat, ν cm^{-1}): 3215, 2922, 1683, 1634, 1266, 757. m/z : calculated for $C_{20}H_{19}N_3O_2Cl_2$ $[M+H]^+$: 404.0927 found 404.0944. Melting point: 134 °C

5.1.8. (Z)-methyl(2-(2-((methylimino)(p-tolyl)methyl)-1H-indol-3-yl)ethyl)carbamate (**2f**)

Compound **2f** was synthesized from **1e** as yellow solid, by following the general procedure. It was purified by column chromatography with ethyl acetate-hexane (3:10) mixture as an eluent. The yield of the reaction was 64%. Following the general procedure, the desired compound **2f** was synthesized from **1e** and was purified with column chromatography with ethyl acetate-hexane (3:10) as eluent. It was generated as yellow solid with yield of 64%. ¹H NMR (400 MHz, DMSO-*d*₆) δ 10.89 (s, 1H), 7.69–7.67 (d, *J* = 8.08 Hz, 1H), 7.58–7.56 (d, *J* = 7.92 Hz, 1H), 7.34–7.32 (m, 2H), 7.16–7.14 (d, *J* = 7.92 Hz, 2H), 7.13–7.08 (m, 2H), 6.97–6.94 (m, 1H), 3.47 (s, 3H), 3.46 (s, 1H), 3.16 (s, 3H), 3.02–2.98 (m, 1H), 2.95–2.90 (m, 2H), 2.39 (s, 3H); ¹³C NMR (100 MHz, DMSO-*d*₆): 163.61, 156.95, 138.71, 136.35, 134.06, 133.16, 129.84, 129.70, 129.61, 128.98, 127.81, 123.57, 119.81, 119.13, 115.18, 112.30, 51.53, 42.20, 24.86, 21.51. IR (neat, *v* cm⁻¹): 3177, 2918, 1698, 1645, 1130. *m/z*: calculated for C₂₁H₂₃N₃O₂ [M+H]⁺: 350.1863 found 350.1895. Melting point: 167 °C

5.1.9. (Z)-methyl(2-(2-((ethylimino)(p-tolyl)methyl)-1H-indol-3-yl)ethyl)carbamate (**2g**)

Compound **2g** was synthesized from **1e** as light yellow solid, by following the general procedure. It was purified by column chromatography with ethyl acetate-hexane (3:10) mixture as an eluent. The yield of the reaction was 88%. ¹H NMR (400 MHz; DMSO-*d*₆) δ 10.75 (s, 1H), 7.69–7.67 (d, *J* = 8.04 Hz, 1H), 7.59–7.57 (d, *J* = 8.00 Hz, 1H), 7.39–7.36 (m, 1H), 7.33–7.31 (d, *J* = 7.76 Hz, 2H), 7.16–7.14 (d, *J* = 7.88 Hz, 2H), 7.11–7.09 (d, *J* = 7.48 Hz, 1H), 6.98–6.94 (t, *J* = 7.2 Hz, 1H), 3.47 (s, 3H), 3.46 (s, 1H); 3.37–3.36 (d, *J* = 7.2 Hz, 1H), 3.21–3.16 (m, 1H), 3.02–2.95 (m, 3H), 2.39 (s, 3H), 1.21–1.17 (t, *J* = 7.2 Hz, 3H); ¹³C NMR (100 MHz; DMSO-*d*₆) δ 156.95, 143.04, 138.73, 136.35, 133.91, 133.32, 129.76, 129.60, 128.91, 127.78, 123.56, 120.19, 119.74, 119.19, 113.19, 112.38, 51.52, 46.98, 42.29, 24.74, 21.48, 16.81. IR (neat, *v* cm⁻¹): 3244, 2922, 1689, 1610, 1135. *m/z*: calculated for C₂₂H₂₅N₃O₂ [M+H]⁺: 364.202 found 364.2032. Melting point: 127 °C

5.1.10. (Z)-methyl(2-(2-((3,4-dimethoxyphenyl)(methylimino)methyl)-1H-indol-3-yl)ethyl)carbamate (**2h**)

Compound **2h** was synthesized from **1f** as yellow solid, by following the general procedure. It was purified by column chromatography with ethyl acetate-hexane (3:10) mixture as an eluent. The yield of the reaction was 84%. ¹H NMR (400 MHz; DMSO-*d*₆) δ 11.45 (s, 1H), 7.76–7.74 (d, *J* = 8.04 Hz, 1H), 7.44–7.40 (m, 2H), 7.38–7.37 (d, *J* = 1.6 Hz, 1H), 7.29–7.25 (m, 1H), 7.20–7.17 (t, *J* = 5.20 Hz, 1H), 7.15–7.12 (d, *J* = 8.36 Hz, 1H), 7.11–7.08 (m, 1H), 3.87 (s, 3H), 3.82 (s, 3H), 3.47 (s, 3H), 3.33 (s, 3H), 3.21–3.19 (d, *J* = 7.4 Hz, 2H), 3.03–3.00 (m, 2H); ¹³C NMR (100 MHz; DMSO-*d*₆) δ 187.61, 157.07, 153.07, 149.00, 136.92, 132.26, 131.50, 127.94, 125.28, 124.47, 120.89, 120.13, 113.13, 112.15, 111.39, 56.25, 55.95, 51.56, 41.94, 25.77. IR (neat, *v* cm⁻¹): 3234, 2919, 1697, 1645, 1137. *m/z*: calculated for C₂₂H₂₅N₃O₄ [M+H]⁺: 396.1918 found 396.1961. Melting point: 147 °C

5.1.11. (Z)-Methyl (2-(2-((methylimino)(phenyl)methyl)-1H-indol-3-yl)ethyl)carbamate (**2i**)

Compound **2i** was synthesized from **1g** as light yellow solid, by following the general procedure. It was purified by column chromatography with ethyl acetate-hexane (3:10) mixture as an eluent. The yield of the reaction was 73%. ¹H NMR (400 MHz; DMSO-*d*₆) δ 10.95 (s, 1H), 7.58–7.51 (m, 4H), 7.38–7.36 (d, *J* = 7.8 Hz, 1H), 7.28–7.27 (d, *J* = 5.2 Hz, 2H), 7.13–7.10 (m, 1H), 7.03 (s, 1H), 6.98–6.96 (d, *J* = 6.92 Hz, 1H), 3.47 (s, 3H), 3.15 (s, 3H), 2.90 (s, 2H), 2.32 (s, 2H); ¹³C NMR (100 MHz; DMSO-*d*₆) δ 163.49, 156.94, 136.38, 136.15, 133.85, 129.35, 129.30, 129.02, 127.79, 123.66, 119.83, 119.15, 115.34, 112.30, 55.38, 51.53, 42.22, 24.811. IR (neat, *v* cm⁻¹): 3251, 2948,

1697, 1640, 1081. *m/z*: calculated for C₂₀H₂₁N₃O₂ [M+H]⁺: 336.1707 found 336.1748. Melting point: 163 °C

5.1.12. (Z)-methyl(2-(2-((3,5-bis(trifluoromethyl)phenyl)(methylimino)methyl)-5-methoxy-1H-indol-3-yl)ethyl)carbamate (**2j**)

Compound **2j** was synthesized from **1h** as yellow solid, by following the general procedure. It was purified by column chromatography with ethyl acetate-hexane (3:10) mixture as an eluent. The yield of the reaction was 91%. ¹H NMR (400 MHz; DMSO-*d*₆) δ 11.09 (s, 1H), 8.25 (s, 1H), 8.06 (s, 2H), 7.31–7.28 (d, *J* = 8.8 Hz, 1H), 7.17–7.16 (d, *J* = 2.08 Hz, 1H), 7.03–7.00 (t, *J* = 5.64 Hz, 1H), 6.86–6.83 (dd, *J*₁ = 2.44 Hz and *J*₂ = 6.36 Hz, 1H), 3.80 (s, 3H), 3.37 (s, 3H), 3.34 (s, 3H), 3.09–3.06 (m, 2H), 2.61–2.57 (t, *J* = 7.04 Hz, 2H); ¹³C NMR (100 MHz; DMSO-*d*₆) δ 160.21, 156.86, 154.01, 141.86, 131.98, 131.10, 130.77, 128.01, 127.76, 127.52, 124.98, 124.10, 122.27, 113.43, 112.99, 112.92, 101.19, 55.84, 51.35, 42.60, 40.96, 25.42. IR (neat, *v* cm⁻¹): 3226, 2950, 1697, 1278, 1075. *m/z*: calculated for C₂₃H₂₁N₃O₃F₆ [M+H]⁺: 502.156 found 502.1612. Melting point: 142 °C

5.1.13. (Z)-methyl(2-(2-((3,5-bis(trifluoromethyl)phenyl)(ethylimino)methyl)-5-methoxy-1H-indol-3-yl)ethyl)carbamate (**2k**)

Compound **2k** was synthesized from **1i** as off white solid, by following the general procedure. It was purified by column chromatography with ethyl acetate-hexane (3:10) mixture as an eluent. The yield of the reaction was 76%. ¹H NMR (400 MHz; DMSO-*d*₆) δ 10.61 (s, 1H), 8.25 (s, 1H), 8.06–8.04 (d, *J* = 9.48 Hz, 2H), 7.26–7.23 (d, *J* = 8.80 Hz, 1H), 7.15 (s, 1H), 7.06 (s, 1H), 6.81–6.78 (dd, *J*₁ = 2.40 Hz and *J*₂ = 6.44 Hz, 1H), 3.75 (s, 3H), 3.46 (s, 3H), 3.29–3.24 (q, *J* = 7.2 Hz, 2H), 3.06–3.03 (t, *J* = 6.00 Hz, 2H), 2.66–2.63 (m, 2H), 1.23–1.97 (t, *J* = 7.2 Hz, 3H); ¹³C NMR (100 MHz; DMSO-*d*₆): 158.27, 156.90, 154.08, 141.89, 138.57, 131.93, 131.54, 131.16, 130.83, 129.79, 127.94, 127.79, 124.98, 122.27, 114.38, 113.30, 112.95, 101.35, 55.89, 55.79, 51.37, 49.33, 25.50, 16.31. IR (neat, *v* cm⁻¹): 3225, 1742, 1697, 1284, 1140. *m/z*: calculated for C₂₄H₂₃N₃O₃F₆ [M+H]⁺: 516.1716 found 516.1748. Melting point: 116 °C

5.1.14. (Z)-methyl(2-(2-((3,5-bis(trifluoromethyl)phenyl)(propylimino)methyl)-5-methoxy-1H-indol-3-yl)ethyl)carbamate (**2l**)

Compound **2l** was synthesized from **1i** as yellow solid, by following the general procedure. It was purified by column chromatography with ethyl acetate-hexane (3:10) mixture as an eluent. The yield of the reaction was 81%. ¹H NMR (400 MHz; DMSO-*d*₆) δ 10.57 (s, 1H), 8.25 (s, 1H), 8.01 (s, 2H), 7.25–7.23 (d, *J* = 8.80 Hz, 1H), 7.14–7.12 (t, *J* = 5.16 Hz, 1H), 7.07–7.06 (d, *J* = 1.72 Hz, 1H), 6.81–6.78 (m, 1H), 3.75 (s, 3H), 3.46 (s, 3H), 3.22–3.18 (t, *J* = 6.76 Hz, 2H), 3.08–3.03 (m, 2H), 2.70–2.67 (t, *J* = 7.04 Hz, 2H), 1.69–1.63 (m, 2H), 0.91–0.87 (t, *J* = 7.44 Hz, 3H); ¹³C NMR (100 MHz; DMSO-*d*₆): 158.53, 153.89, 138.67, 131.93, 129.23, 128.01, 127.75, 113.34, 55.89, 55.75, 51.45, 29.44, 24.33, 24.09, 12.45. IR (neat, *v* cm⁻¹): 3375, 2921, 1742, 1622, 1276, 1128. *m/z*: calculated for C₂₅H₂₅N₃O₃F₆ [M+H]⁺: 530.1873 found 530.1911. Melting point: 118 °C

5.1.15. (Z)-methyl(2-(2-((methylimino)(4-nitrophenyl)methyl)-1H-indol-3-yl)ethyl)carbamate (**2m**)

Compound **2m** was synthesized from **1j** as bright yellow solid, by following the general procedure. It was purified by column chromatography with ethyl acetate-hexane (3:10) mixture as an eluent. The yield of the reaction was 65%. ¹H NMR (400 MHz; DMSO-*d*₆) δ 11.56 (s, 1H), 8.41–8.38 (d, *J* = 8.72 Hz, 2H), 7.97–7.95 (d, *J* = 8.76 Hz, 2H), 7.77–7.75 (d, *J* = 8.12 Hz, 1H), 7.44–7.42 (d, *J* = 8.28 Hz, 1H), 7.34–7.30 (m, 1H), 7.16–7.10 (m, 2H), 3.45 (s, 3H), 3.33 (s, 3H), 3.17–3.12 (m, 2H), 2.95–2.91 (m, 2H); ¹³C NMR

(100 MHz; DMSO- d_6) δ 187.47, 157.04, 149.61, 145.02, 137.64, 131.38, 130.32, 126.53, 124.26, 121.39, 120.55, 113.31, 51.57, 41.64, 25.87. IR (neat, ν cm^{-1}): 3213, 2921, 1688, 1631, 1519, 1106. m/z: calculated for $\text{C}_{20}\text{H}_{20}\text{N}_4\text{O}_4$ [M-H]⁻ 368.1171 found 368.1154. Melting point: 158 °C

5.1.16. (Z)-methyl(2-(2-((ethylimino)(4-nitrophenyl)methyl)-1H-indol-3-yl)ethyl)carbamate (**2n**)

Compound **2n** was synthesized from **1j** as bright yellow solid, by following the general procedure. It was purified by column chromatography with ethyl acetate-hexane (3:10) mixture as an eluent. The yield of the reaction was 73%. ¹H NMR (400 MHz; DMSO- d_6) δ 10.90 (s, 1H), 8.37-8.34 (d, J = 8.56 Hz, 2H), 7.62-7.60 (m, 3H), 7.38 (s, 1H), 7.17-7.10 (m, 2H), 7.01-6.97 (m, 1H), 3.47 (s, 3H), 3.30 (s, 1H), 3.28 (s, 1H), 2.94-2.90 (m, 2H), 2.39-2.37 (m, 2H), 1.23-1.22 (d, J = 2.42 Hz, 3H); ¹³C NMR (100 MHz; DMSO- d_6): 159.79, 148.19, 143.02, 136.55, 132.76, 129.39, 124.54, 124.05, 119.83, 112.42, 51.50, 47.14, 29.44, 16.63, 16.41. IR (neat, ν cm^{-1}): 3253, 2921, 1689, 1519, 1042. m/z: calculated for $\text{C}_{21}\text{H}_{22}\text{N}_4\text{O}_4$ [M+H]⁺: 395.1714 found 395.1731. Melting point: 157 °C

5.1.17. (Z)-methyl(2-(2-((4-bromothiophen-2-yl)(methylimino)methyl)-1H-indol-3-yl)ethyl)carbamate (**2o**)

Compound **2o** was synthesized from **1k** as yellow solid, by following the general procedure. It was purified by column chromatography with ethyl acetate-hexane (3:10) mixture as an eluent. The yield of the reaction was 71%. ¹H NMR (400 MHz; DMSO- d_6) δ 11.28 (s, 1H), 7.80 (s, 1H), 7.64 (s, 1H), 7.36 (s, 1H), 7.17-7.09 (m, 3H), 6.79 (s, 1H), 3.41 (s, 3H), 3.21 (s, 3H), 3.12 (s, 2H), 2.67 (s, 2H); ¹³C NMR (100 MHz; DMSO) δ 156.97, 147.35, 136.72, 131.74, 127.88, 127.40, 126.98, 122.73, 119.62, 112.41, 112.15, 109.21, 51.53, 41.55, 41.23, 25.68. IR (neat, ν cm^{-1}): 3278, 2919, 1694, 1608, 1137, 583. m/z: calculated for $\text{C}_{18}\text{H}_{18}\text{N}_3\text{O}_2\text{SBr}$ [M+H]⁺: 422.0356 and 420.0376 found 422.0406 and 420.0425. Melting point: 99 °C

5.1.18. (Z)-methyl(2-(2-((2,6-difluorophenyl)(methylimino)methyl)-1H-indol-3-yl)ethyl)carbamate (**2p**)

Compound **2p** was synthesized from **1l** as light yellow solid, by following the general procedure. It was purified by column chromatography with ethyl acetate-hexane (3:10) mixture as an eluent. The yield of the reaction was 69%. ¹H NMR (400 MHz; DMSO- d_6) δ 11.10 (s, 1H), 7.68-7.65 (m, 1H), 7.62-7.60 (d, J = 8.04 Hz, 1H), 7.39-7.37 (d, J = 8.16 Hz, 1H), 7.32-7.28 (t, J = 7.96 Hz, 2H), 7.17-7.14 (m, 1H), 7.07 (s, 1H), 7.01-6.98 (t, J = 7.44 Hz, 1H), 3.49 (s, 3H), 3.20 (s, 3H), 2.98-2.94 (m, 2H), 2.54-2.51 (d, J = 8.16 Hz, 2H); ¹³C NMR (100 MHz; DMSO): 160.21, 157.76, 157.68, 156.99, 152.27, 136.57, 133.09, 132.99, 132.89, 132.40, 128.95, 124.12, 120.00, 119.45, 115.34, 112.98, 112.75, 112.37, 112.15, 51.55, 42.04, 40.74, 25.03. IR (neat, ν cm^{-1}): 3189, 2919, 1688, 1622, 1146, 1048. m/z: calculated for $\text{C}_{20}\text{H}_{19}\text{N}_3\text{O}_2\text{F}_2$ [M+H]⁺: 372.1518 found 372.1558. Melting point: 122 °C.

5.1.19. Representative experimental procedures for the synthesis of tetrahydro- β -carboline-diketopiperazine hybrids (**3** & **4**)

Step-1: To the solution of tryptophan methyl ester (1 equiv.) in dichloromethane (DCM), substituted benzaldehydes (0.8 equiv.) with trifluoroacetic acid (1.5 equiv.) were added and allowed to stir at room temperature for 24 h. After completion of reaction, reaction mixture was concentrated under reduced pressure and quenched with saturated solution of 5% sodium bicarbonate (NaHCO_3). It was then recrystallized with minimum amount of DCM to obtain crude product which was taken to the next step without purification.

Step-2: To the above crude compound (1 equiv.) and sodium bicarbonate (NaHCO_3) (1.2 equiv.) in chloroform (CHCl_3) chloroacetyl chloride (2.4 equiv.) was added dropwise at 0 °C. The

reaction mixture was stirred at room temperature under nitrogen atmosphere for 3 h. After completion of reaction it was monitored by TLC and the reaction mixture was diluted by CHCl_3 followed by washing with saturated solution of NaHCO_3 , brine, dried over Na_2SO_4 , which was evaporated under reduced pressure to obtained crude product which was taken to the next step without purification.

Step-3: To the solution of the above crude compound (1 equiv.) appropriate amine (5 equiv.) was added in ethanol and was stirred at 50 °C for 24 h. It was then concentrated under reduced pressure after completion of reaction. Purification of the crude product was done with column chromatography keeping ethyl acetate-hexane as eluent.

Step-4: To the solution of above compound in acetonitrile (1 equiv.), iodine (0.3 equiv.), TBHP (4 equiv.) was taken and was stirred at 60 °C for 4 h. Once the reaction is complete it was evaporated under reduced pressure to obtained crude product which was purified by column chromatography with ethyl acetate-hexane as eluent. The purified compound was dissolved in methanol and at 0 °C NaNH_4 (2 equiv.) was added. The desired compound was obtained after stirring for 2 h.

5.1.20. 1-Benzyl-3-((2-(hydroxy(2-nitrophenyl)methyl)-1H-indol-3-yl)methyl)piperazine-2,5-dione (**3**)

Following the general procedure, the desired compound **3** was synthesized from tryptophan methyl ester (500 mg, 2.29 mmol) and 2-nitrobenzaldehyde (346 mg, 1.83 mmol) and then nitrogen of the resulting tetrahydro- β -carboline was protected with DKP group having benzyl protection at nitrogen of DKP which then formed ring opened product in presence of iodine and TBHP. This compound was reduced and purified by column chromatography with ethyl acetate-hexane as eluent and was obtained as pale yellow solid with yield of 75%. ¹H NMR (400 MHz; CDCl_3): δ 8.39 (s, 1H), 7.85 (d, J = 8 Hz, 1H), 7.64 (d, J = 8 Hz, 1H), 7.58 (d, J = 8 Hz, 2H), 7.45 (t, J = 8 Hz, 1H), 7.29 (d, J = 8 Hz, 1H), 7.23 (t, J = 4 Hz, 3H), 7.19 (d, J = 8 Hz, 1H), 7.13 (t, J = 8 Hz, 1H), 6.98 (m, 3H), 6.72 (s, 1H), 4.93 (d, J = 16 Hz, 2H), 4.44 (s, 1H), 3.59 (dd, J = 4, 16 Hz, 1H), 3.34 (s, 1H), 3.30 (d, J = 8 Hz, 1H), 3.27 (d, J = 4 Hz, 1H), 2.47 (d, J = 16 Hz, 1H); ¹³C NMR (100 MHz; CDCl_3): δ 168.43, 166.41, 148.26, 136.51, 135.71, 134.77, 133.42, 128.92, 128.65, 128.47, 128.09, 127.75, 124.86, 123.12, 120.25, 119.58, 111.35, 106.71, 64.74, 56.28, 49.47, 29.83. m/z: calculated for $\text{C}_{27}\text{H}_{24}\text{N}_4\text{O}_5$ [M-H]⁻: 483.1674 found 483.1680.

5.1.21. 1-Benzyl-3-((2-(hydroxy(phenyl)methyl)-1H-indol-3-yl)methyl)piperazine-2,5-dione (**4**)

Following the general procedure, the desired compound **4** was synthesized from tryptophan methyl ester (500 mg, 2.29 mmol) and benzaldehyde (0.19 ml, 1.83 mmol) and then nitrogen of the resulting tetrahydro- β -carboline was protected with DKP group having benzyl protection at nitrogen of DKP which then formed ring opened product in presence of iodine and TBHP. This compound was reduced and purified by column chromatography with ethyl acetate-hexane as eluent and was obtained as pale yellow solid with yield of was obtained as pale yellow solid with yield of 80%. ¹H NMR (400 MHz; CDCl_3): δ 8.07 (s, 1H), 7.38 (d, J = 8 Hz, 1H), 7.35-7.32 (m, 4H), 7.31-7.28 (m, 4H), 7.24 (s, 1H), 7.17-7.10 (m, 4H), 7.09 (s, 1H), 6.08 (s, 1H), 4.61 (d, J = 20 Hz, 1H), 4.38 (s, 1H), 4.34 (d, J = 12 Hz, 2H), 3.61 (d, J = 20 Hz, 2H), 3.35 (d, J = 20 Hz, 1H), 3.25 (dd, J = 12, 20 Hz, 1H); ¹³C NMR (100 MHz; CDCl_3): δ 166.12, 166.10, 141.33, 138.27, 135.56, 134.86, 129.07, 128.86, 128.85, 128.40, 128.39, 128.26, 126.39, 111.42, 106.84, 67.87, 56.05, 49.73, 48.83, 29.85, 29.69. m/z: calculated for $\text{C}_{27}\text{H}_{23}\text{N}_3\text{O}_3$ [M+H]⁺: 438.1812 found 438.1816.

5.1.22. Oxidative ring opening for the synthesis of (5)

5.1.22.1. Methyl (2-(2-(4-chlorobenzoyl)-1H-indol-3-yl)ethyl)carbamate (5). Compounds **1a** (1 equiv.), molecular iodine (0.3 equiv.) and *tert*-butyl hydroperoxide (4 equiv.) was taken in THF and was stirred at 40 °C temperature for 4 h. The reaction was monitored by TLC, once the reaction was completed the reaction mixture was cooled to room temperature and quenched with saturated solution of sodium thiosulphate in water and extracted with ethyl acetate. The organic layer was dried over anhydrous $\text{Na}_2\text{S}_2\text{O}_4$, and evaporated under reduced pressure. The crude product was purified with column chromatography with ethyl acetate-hexane (3:10) as eluent and generated as yellow solid with yield of 82%. ^1H NMR (400 MHz; DMSO- d_6): 11.48 (s, 1H); 7.79–7.75 (m, 3H); 7.66–7.64 (d, $J = 4$, 2H); 7.44–7.42 (d, $J = 8$ Hz, 1H); 7.32–7.28 (m, 1H); 7.19–7.16 (t, $J = 6$ Hz, 1H); 7.13–7.09 (m, 1H); 3.46 (s, 3H); 3.21–3.16 (m, 2H); 3.03–2.99 (t, $J = 8$ Hz, 2H). ^{13}C NMR (100 MHz; DMSO- d_6): 187.77, 157.07, 138.01, 137.52, 137.29, 131.67, 131.30, 129.18, 127.99, 125.94, 121.59, 121.59, 121.16, 120.36, 113.24, 51.56, 41.79, 25.75. m/z : calculated for $\text{C}_{19}\text{H}_{17}\text{ClN}_2\text{O}_3[\text{M}+\text{H}]^+$: 357.1000 found 357.1034.

5.1.23. Plasmodium falciparum culture

Human malarial parasite *Plasmodium falciparum* was cultured in human O positive erythrocytes in RPMI 1640 medium supplemented with 0.2% NaHCO_3 , 0.5% albumin, 10 $\mu\text{g}/\text{ml}$ gentamicin sulfate and 50 $\mu\text{g}/\text{ml}$ hypoxanthine at 37 °C in a gas mixture (90% nitrogen, 5% carbon dioxide and 5% oxygen) environment. Parasite culture was maintained at 5% hematocrit. Microscopic examination of giemsa-stained parasite infected blood smears was used to determine the parasitemia and parasite stages. Synchronization of parasite culture was carried out using sorbitol method [22].

5.1.24. Plasmodium falciparum growth inhibition assay

To detect the inhibitory effect of synthesized compounds, synchronized parasite culture (of 3D7 or RKL9 strain) of ring stage at 1% parasitemia cultured in 12-well plates were treated with compounds at 10 μM concentration for 48 h. DMSO was used as control. Slide smear of infected erythrocytes were prepared at regular intervals (0, 12, 24, 36 and 48 h post treatment) to analyze the parasitemia and morphology of parasites were examined using giemsa-staining method [22]. Similarly, mixed stage parasite culture were treated either with melatonin alone or melatonin with luzindole or compound **2j**. Stage progression and parasitemia were monitored by giemsa staining of infected blood smears.

5.1.25. Molecular modelling and docking

Human MT1 sequence was modelled using homology modelling approach considering the human $\beta(2)$ adrenergic receptor ($\beta(2)\text{AR}$) protein (PDB ID: 3P0G) as a plausible template. Earlier $\beta(2)\text{AR}$ was used as a template for MT1 structure prediction [34]. However, we have recreated the human MT1 three-dimensional (3D) using MAFFT [35] based alignment and the MODELLER software [35]. Output models were ranked on the basis of DOPE score and were validated using structure validation programs, such as Verify 3D and RAMPAGE [31,36]. Some regions of the validated MT1 models were further refined by loop modelling using MODELLER in order to get models with least stereo chemical violations.

Three-dimensional (3D) coordinates and their respective conformers of compounds **2j** and **2k** were generated *in-silico* modelling using FROG2 software [37]. Molecular docking of top 10 energetically stable conformers were docked at the known substrate/inhibitor binding site of the MT1 structure using the GOLD (Genetic Optimization for Ligand Docking) package [37]. GOLD software optimizes the fitness score of many possible docking solutions using a genetic algorithm. The parameters used in the docking cycles included population size (10), selection pressure

(1.100000), number of operations (100,000), number of islands (5), niche size (2), crossover weight (95), mutate weight (95), and migrate weight (10). All the docking solutions from various conformers were pooled together for clustering analysis based on their root mean square deviation (RMSD) representing structural similarity. Sub-clusters with minimum of 3 solutions with RMSD < 2 Å with the highest docking scores were considered for further analysis. Top 3 scoring solutions (poses) from the largest cluster were selected based on the docking score and compared. Further, ΔG of the binding was estimated by MOPAC software [38]. Protein-ligand interactions from the representative docking complexes were identified by the LigPlot program [39].

5.2. Binding to melatonin receptor MTNR1

Compounds **2g**, **j** and **k** were incubated with 5 ng/mL MTNR1 receptor provided by Cloudclone Melatonin Receptor Assay Kit at a concentration of 500 nM, 1 and 5 μM . After 1 h of incubation secondary antibody was added. Next unbound antibody was washed away by wash buffer and then HRP conjugated antibody was added. After thirty minutes of incubation, substrate TMB was added followed by the addition of stop solution to prevent the peroxidase reaction. O.D. was measured with a Biorad micro elisa plate reader (iMark) at wavelength 450 nm.

5.2.1. Screening of potent compounds against HepG2 cell line

Cytotoxicity assay. MTT assay (a colorimetric assay to assess cell metabolic activity) was performed to check the growth inhibitory effects of the ligands on human cancer cell line. Accordingly cultured HepG2 cells were seeded on a 96-well microtiter plate (1×10^4 cells/mL) and treated with varying concentrations (0 μM –50 μM) of the ligands (**2g**, **i**, **j**, **k** and **p**) for 48 h. After 48 h, 50 μL of the MTT solution (2 mg/mL) was added to each well followed by the dissolution of the purple formazan crystals formed in 100 μL of DMSO. Then, the absorbance was measured at 595 nm in an enzyme-linked immunosorbent assay reader (Multiskan EX, Labsystems). Data were calculated as the percentage of inhibition by the following formula [40].

%inhibition = $(100 - (A_t/A_s) * 100)$ % where A_t and A_s are the absorbance of the test substances and solvent control, respectively.

5.2.2. Stability of the compound 2g, i, j, k and p

Stability tests of compounds (**2g**, **2i**, **2j**, **2k**, **2p**) in physiological conditions (simulated stomach acid & physiological buffer). A 100 μL portion of 1.0 mg stock solution (in acetonitrile) of **2g**, **2i**, **2j**, **2k**, **2p** was added to a) 1.0 mL of freshly prepared 0.01 N HCl aqueous solution (pH = 2.0) and b) 1.0 mL of freshly prepared phosphate buffer solution (pH = 7.4) respectively. The resulting mixtures were maintained at 37 °C. The reaction mixtures were analyzed by HPLC at different interval of time starting from 0 h till 24 h.

Acknowledgement

We thank Shiv Nadar University for the financial support.

Appendix A. Supplementary data

Supplementary data to this article can be found online at <https://doi.org/10.1016/j.ejmech.2019.02.019>.

References

- [1] S.I. Hay, C.A. Guerra, A.J. Tatem, A.M. Noor, R.W. Snow, The global distribution and population at risk of malaria: Past, present, and future, *Lancet Infect. Dis.* 4

- (2004) 327–336.
- [2] N.J. White, Assessment of the pharmacodynamic properties of antimalarial drugs in vivo, *Antimicrob. Agents Chemother.* 41 (1997) 1413–1422.
 - [3] C. Chang, T. Lin-Hua, C. Jantanavivat, Studies on a new antimalarial compound: Pyronaridine, *Trans. R. Soc. Trop. Med. Hyg.* 86 (1992) 7–10.
 - [4] S. Toovey, A. Jamieson, G. Nettleton, Successful co-artemether (artemether-lumefantrine) clearance of *falciparum* malaria in a patient with severe cholera in Mozambique, *Trav. Med. Infect. Dis.* 1 (2003) 177–179.
 - [5] V. Duru, B. Witkowski, D. Menard, *Plasmodium falciparum* resistance to artemisinin derivatives and piperazine: A major challenge for malaria elimination in Cambodia, *Am. J. Trop. Med. Hyg.* 95 (2016) 1228–1238.
 - [6] R.E. Martin, R.V. Marchetti, A.I. Cowan, S.M. Howitt, S. Bröer, K. Kirk, Chloroquine transport via the malaria parasite's chloroquine resistance transporter, *Science* 325 (2009) 1680–1682.
 - [7] P. Schlagenhauf, Mefloquine for malaria chemoprophylaxis 1992–1998: A review, *Trav. Med.* 6 (1999) 122–123.
 - [8] D.J. Lange, P.M. Andersen, R. Reman, S. Marklund, D. Benjamin, Pyrimethamine decreases levels of SOD1 in leukocytes and cerebrospinal fluid of ALS patients: A phase I pilot study, *Amyotroph. Lateral Scler. Frontotemporal Degeneration* 14 (2013) 199–204.
 - [9] M.N. Dohn, W.G. Weinberg, R.A. Torres, S.E. Follansbee, P.T. Caldwell, J.D. Scott, J.C. Gathe, D.P. Haghghat, J.H. Sampson, J. Spotkov, S.C. Deresinski, R.D. Meyer, D.J. Lancaster, Oral atovaquone compared with intravenous pentamidine for *Pneumocystis carinii* pneumonia in patients with AIDS, *Ann. Intern. Med.* 121 (1994) 174–180.
 - [10] E. Worrall, S. Basu, K. Hanson, Is malaria a disease of poverty? A review of the literature, *Trop. Med. Int. Health* 10 (2005) 1047–1059.
 - [11] T.M. Tran, B. Samal, E. Kirkness, P.D. Crompton, Systems immunology of human malaria, *Trends Parasitol.* 28 (2012) 248–257.
 - [12] E.L. Flannery, A.K. Chatterjee, E.A. Winzler, Antimalarial drug discovery: Approaches and progress towards new medicines, *Nat. Rev. Microbiol.* 11 (2013) 849–862.
 - [13] D.I. Ugwu, U.C. Okoro, P.O. Ukoha, A. Ibezim, S. Okafor, N.M. Kumar, Synthesis, characterization, molecular docking and in vitro antimalarial properties of new carboxamides bearing sulphonamide, *Eur. J. Med. Chem.* 135 (2017) 349–369.
 - [14] P.N. Kalaria, S.C. Karad, D.K. Raval, A review on diverse heterocyclic compounds as the privileged scaffolds in antimalarial drug discovery, *Eur. J. Med. Chem.* 158 (2018) 917–936.
 - [15] A.A. Bekhit, M.N. Saudi, A.M.M. Hassan, S.M. Fahmy, T.M. Ibrahim, D. Ghareeb, A.M. El-Seidy, S.N. Nasralla, A. El-Din, A. Bekhit, Synthesis, *in silico* experiments and biological evaluation of 1,3,4-trisubstituted pyrazole derivatives as antimalarial agents, *Eur. J. Med. Chem.* 163 (2019) 353–366.
 - [16] G. Kumar, O. Tanwar, J. Kumar, M. Akhter, S. Sharma, C.R. Pillai, Md. M. Alam, M.S. Zama, Pyrazole-pyrazoline as promising novel antimalarial agents: A mechanistic study, *Eur. J. Med. Chem.* 149 (2018) 139–147.
 - [17] G.C. Brandão, F.C.R. Missias, L.M. Arantes, L.F. Soares, K.K. Roy, R.J. Doerksen, A.B. de Oliveira, G.R. Pereira, Antimalarial naphthoquinones. Synthesis via click chemistry, *in vitro* activity, docking to PfDHODH and SAR of lapachol-based compounds, *Eur. J. Med. Chem.* 145 (2018) 191–205.
 - [18] V. Gayam, S. Ravi, Cinnamoylated chloroquine analogues: A new structural class of antimalarial agents, *Eur. J. Med. Chem.* 135 (2017) 382–391.
 - [19] D. Gonçalves, P. Hunziker, Transmission-blocking strategies: The roadmap from laboratory bench to the community, *Malar. J.* 15 (2016) 95–107.
 - [20] S.S. Yazdani, P. Mukherjee, V.S. Chauhan, C.E. Chitnis, Immune responses to asexual blood-stages of malaria parasites, *Curr. Mol. Med.* 6 (2006) 187–203.
 - [21] R. Hardeland, S.R. Pandi-Perumal, D.P. Cardinali, Melatonin, *Int. J. Biochem. Cell Biol.* 3 (2006) 313–316.
 - [22] V. Srinivasan, M. Mohamed, H. Kato, Melatonin in bacterial and viral infections with focus on sepsis: A review, *Recent Pat. Endocr. Metab. Immune Drug Discov.* 6 (2012) 30–39.
 - [23] V. Srinivasan, D.W. Spence, A. Moscovitch, S.R. Pandi-Perumal, I. Trakht, G.M. Brown, D.P. Cardinali, Malaria: Therapeutic implications of melatonin, *J. Pineal Res.* 48 (2010) 1–8.
 - [24] C.T. Hotta, M.L. Gazarini, F.H. Beraldo, F.P. Varotti, C. Lopes, R.P. Markus, T. Pozzan, C.R.S. Garcia, Calcium-dependent modulation by melatonin of the circadian rhythm in malarial parasite, *Nat. Cell Biol.* 2 (2000) 466–468.
 - [25] D.C. Schuck, A.K. Jordão, M. Nakabashi, A.C. Cunha, V.F. Ferreira, C.R.S. Garcia, Synthetic indole and melatonin derivatives exhibit antimalarial activity on the cell cycle of the human malaria parasite *Plasmodium falciparum*, *Eur. J. Med. Chem.* 75 (2014) 375–382.
 - [26] M. Guha, P. Maity, V. Choubey, K. Mitra, R.J. Reiter, U. Bandyopadhyay, Melatonin inhibits free radical-mediated mitochondrial-dependent hepatocyte apoptosis and liver damage induced during malarial infection, *J. Pineal Res.* 43 (2007) 372–381.
 - [27] A.M. Mathes, D. Kubulus, L. Waibel, J. Weiler, P. Heymann, B. Wolf, H. Rensing, Selective activation of melatonin receptors with ramelteon improves liver function and hepatic perfusion after hemorrhagic shock in rat, *Crit. Care Med.* 36 (2008) 2863–2870.
 - [28] M.L. Dubocovich, Luzindole (N-0774): A novel melatonin receptor antagonist, *J. Pharmacol. Exp. Therapeut.* 246 (1998) 902–910.
 - [29] L.S. Fernandez, M.S. Buchanan, A.R. Carroll, Y.J. Feng, R.J. Quinn, V.M. Avery, A.-C. flinderoles, Antimalarial bis-indole alkaloids from *Flindersia* species, *Org. Lett.* 11 (2009) 329–332.
 - [30] J. Chauhan, T. Luthra, S. Sen, Iodine-catalyzed metal-free oxidative ring opening of 1-Aryltetrahydro- β -carboline: Facile synthesis of C-2 aroyl and aryl methanimino indole derivatives, *Eur. J. Org. Chem.* 34 (2018) 4776–4786.
 - [31] A. Šali, T.L. Blundell, Comparative protein modelling by satisfaction of spatial restraints, *J. Mol. Biol.* 234 (1993) 779–815.
 - [32] S.C. Lovell, I.W. Davis, W.B. Arendall III, P.I.W. de Bakker, J.M. Word, M.G. Prisant, J.S. Richardson, D.C. Richardson, Structure validation by α geometry: Φ , Ψ and $C\beta$ deviation, *Proteins Struct. Funct. Genet.* 50 (2003) 437–450.
 - [33] R.A. Laskowski, M.B. Swindells, LigPlot+: Multiple ligand-protein interaction diagrams for drug discovery, *J. Chem. Inf. Model.* 51 (2011) 2778–2786.
 - [34] S. Rivara, D. Pala, A. Lodola, M. Mor, V. Lucini, S. Dugnani, F. Scaglione, A. Bedini, S. Lucarini, G. Tarzia, G. Spadoni, MT1-selective melatonin receptor ligands: Synthesis, pharmacological evaluation, and molecular dynamics investigation of N-[(3-O-substituted)anilino]alkyl]amides, *ChemMedChem* 7 (2012) 1954–1964.
 - [35] (a) J.U. Bowie, R. Lüthy, D. Eisenberg, A method to identify protein sequences that fold into a known three-dimensional structure, *Science* 253 (1991) 164–170;
(b) K. Katoh, K. Misawa, K. Kuma, T. Miyata, MAFFT: A novel method for rapid multiple sequence alignment based on fast Fourier transform, *Nucleic Acids Res.* 30 (2002) 3059–3066.
 - [36] R.A. Friesner, J.L. Banks, R.B. Murphy, T.A. Halgren, J.J. Klicic, D.T. Mainz, M.P. Repasky, E.H. Knoll, M. Shelley, J.K. Perry, D.E. Shaw, P. Francis, P.S. Shenkin, Glide: A new approach for rapid, accurate docking and scoring. 1. Method and assessment of docking accuracy, *J. Med. Chem.* 47 (2004) 1739–1749.
 - [37] Accelrys Software Inc., Discovery Studio Modeling Environment, Release 4.0, Accelrys Software Inc., San Diego, 2007.
 - [38] MOPAC, James J.P. Stewart, *Stewart Computational Chemistry*, Colorado Springs, CO, USA, 2010. <http://OpenMOPAC.net>.
 - [39] R.A. Laskowski, M.B. Swindells, LigPlot+: multiple ligand-protein interaction diagrams for drug discovery, *J. Chem. Inf. Model.* 51 (2011) 2778–2786.
 - [40] (a) S. Mukherjee, B.R. Acharya, B. Bhattacharyya, G. Chakrabarti, Genistein arrests cell cycle progression of A549 cells at the G2/M phase and depolymerizes interphase microtubules through binding to a unique site of tubulin, *Biochemistry* 49 (2010) 1702–1712;
(b) D. Sładowski, S.J. Steer, R.H. Clothier, M. Balls, Detection of intracellular cytokines by flow cytometry, *J. Immunol. Methods* 157 (1993) 203–207.